

A MATRIX-ORIENTED POD-DEIM ALGORITHM APPLIED TO SEMILINEAR MATRIX DIFFERENTIAL EQUATIONS *

GERHARD KIRSTEN[†] AND VALERIA SIMONCINI[‡]

Abstract. We are interested in numerically approximating the solution $\mathbf{U}(t)$ of the large dimensional semilinear matrix differential equation $\dot{\mathbf{U}}(t) = \mathbf{A}\mathbf{U}(t) + \mathbf{U}(t)\mathbf{B} + \mathcal{F}(\mathbf{U}, t)$, with appropriate starting and boundary conditions, and $t \in [0, T_f]$. In the framework of the Proper Orthogonal Decomposition (POD) methodology and the Discrete Empirical Interpolation Method (DEIM), we derive a novel matrix-oriented reduction process leading to an effective, structure aware low order approximation of the original problem. The reduction of the nonlinear term is also performed by means of a fully matricial interpolation using left and right projections onto two distinct reduction spaces, giving rise to a new two-sided version of DEIM. By maintaining a matrix-oriented reduction, we are able to employ first order exponential integrators at negligible costs. Numerical experiments on benchmark problems illustrate the effectiveness of the new setting.

Key words. Proper orthogonal decomposition, Discrete empirical interpolation method, Semilinear matrix differential equations, Exponential integrators.

AMS subject classifications. 37M99, 15A24, 65N06, 65F30

1. Problem description. We are interested in numerically approximating the solution $\mathbf{U}(t) \in \mathcal{S}$ to the following semilinear matrix differential equation

$$(1.1) \quad \dot{\mathbf{U}}(t) = \mathbf{A}\mathbf{U}(t) + \mathbf{U}(t)\mathbf{B} + \mathcal{F}(\mathbf{U}, t), \quad \mathbf{U}(0) = \mathbf{U}_0,$$

where $\mathbf{A} \in \mathbb{R}^{n_x \times n_x}$, $\mathbf{B} \in \mathbb{R}^{n_y \times n_y}$, and $t \in [0, T_f] = \mathcal{T} \subset \mathbb{R}$, equipped with appropriate boundary conditions. The function $\mathcal{F} : \mathcal{S} \times \mathcal{T} \rightarrow \mathbb{R}^{n_x \times n_y}$ is a sufficiently regular nonlinear function that can be evaluated elementwise, and \mathcal{S} is a functional space containing the sought after solution.

The problem (1.1) arises for instance in the discretization of two-dimensional partial differential equations of the form

$$(1.2) \quad u_t = \ell(u) + f(u, t), \quad u = u(x, y, t) \quad \text{with } (x, y) \in \Omega \subset \mathbb{R}^2, t \in \mathcal{T},$$

and given initial condition $u(x, y, 0) = u_0(x, y)$, for certain choices of the physical domain Ω . The differential operator ℓ is linear in u , typically a second order operator in the space variables, while $f : S \times \mathcal{T} \rightarrow \mathbb{R}$ is a nonlinear function, where S is an appropriate space with $u \in S$. Time dependent equations of type (1.2) arise in biology and ecology, chemistry and physics, where the interest is in monitoring the time evolution of a complex phenomenon; see, e.g., [38],[39],[45],[51], and references therein.

We develop a matrix-oriented POD-DEIM order reduction strategy for the problem (1.1) that leads to a semilinear *matrix* differential equation with the same structure as (1.1), but of significantly reduced dimension. More precisely, we determine an approximation to $\mathbf{U}(t)$ of the type

$$(1.3) \quad \mathbf{V}_{\ell, U} \mathbf{Y}_k(t) \mathbf{W}_{r, U}^\top, \quad t \in [0, T_f],$$

*This version dated May 26, 2021

[†]Dipartimento di Matematica, Università di Bologna, Piazza di Porta S. Donato, 5, I-40127 Bologna, Italy, (gerhard.kirsten2@unibo.it)

[‡]Dipartimento di Matematica and AM², Università di Bologna, Piazza di Porta S. Donato, 5, I-40127 Bologna, Italy; and IMATI-CNR, Pavia Italy (valeria.simoncini@unibo.it).

where $\mathbf{V}_{\ell,U} \in \mathbb{R}^{n \times k_1}$ and $\mathbf{W}_{r,U} \in \mathbb{R}^{n \times k_2}$ are matrices to be determined, independent of time. Here $k_1, k_2 \ll n$ and we let $k = (k_1, k_2)$. The function $\mathbf{Y}_k(t)$ is determined as the numerical solution to the following *reduced* semilinear matrix differential problem

$$(1.4) \quad \begin{aligned} \dot{\mathbf{Y}}_k(t) &= \mathbf{A}_k \mathbf{Y}_k(t) + \mathbf{Y}_k(t) \mathbf{B}_k + \widehat{\mathcal{F}_k(\mathbf{Y}_k, t)} \\ \mathbf{Y}_k(0) &= \mathbf{Y}_k^{(0)} := \mathbf{V}_{\ell,U}^\top \mathbf{U}_0 \mathbf{W}_{r,U}, \end{aligned}$$

with $\mathbf{A}_k = \mathbf{V}_{\ell,U}^\top \mathbf{A} \mathbf{V}_{\ell,U}$, $\mathbf{B}_k = \mathbf{W}_{r,U}^\top \mathbf{B} \mathbf{W}_{r,U}$, and $\widehat{\mathcal{F}_k(\mathbf{Y}_k, t)}$ is a matrix-oriented DEIM approximation to

$$(1.5) \quad \mathcal{F}_k(\mathbf{Y}_k, t) = \mathbf{V}_{\ell,U}^\top \mathcal{F}(\mathbf{V}_{\ell,U} \mathbf{Y}_k \mathbf{W}_{r,U}^\top, t) \mathbf{W}_{r,U}.$$

Standard procedures for (1.1) employ a vector-oriented approach: semi-discretization of (1.2) in space leads to the following system of ordinary differential equations (ODEs)

$$(1.6) \quad \dot{\mathbf{u}}(t) = \mathbf{L} \mathbf{u}(t) + \mathbf{f}(\mathbf{u}, t), \quad \mathbf{u}(0) = \mathbf{u}_0.$$

For $t > 0$, the vector $\mathbf{u}(t)$ contains the representation coefficients of the sought after solution in the chosen discrete space, $\mathbf{L} \in \mathbb{R}^{N \times N}$ accounts for the discretization of the linear differential operator ℓ and \mathbf{f} is evaluated componentwise at $\mathbf{u}(t)$.

The discretization of (1.2) can directly lead to the form (1.1) whenever ℓ is a second order differential operator with separable coefficients and a tensor basis is used explicitly or implicitly for its discretization, such as finite differences on structured grids, certain spectral methods, isogeometric analysis, etc. In a tensor space discretization, for instance, the discretization of $\ell(u)$ yields the operator $\mathbf{U} \mapsto \mathbf{A} \mathbf{U} + \mathbf{U} \mathbf{B}$, where the matrices \mathbf{A} and \mathbf{B} approximate the second order derivatives in the x - and y -directions, respectively, using n_x and n_y discretization nodes¹. We aim to show that by sticking to the matrix formulation of the problem throughout the computation - including the reduced model - major advantages in terms of memory allocations, computational costs and structure preservation can be obtained.

For $\mathcal{F} \equiv 0$, the equation (1.1) simplifies to the differential Sylvester equation, for which reduction methods have shown to be competitive; see, e.g., [10] and references therein. Our approach generalizes to the semilinear case a matrix-oriented projection methodology successfully employed in this linear and quadratic contexts [35]. A challenging difference lies in the selection and construction of the two matrices $\mathbf{V}_{\ell,U}$, $\mathbf{W}_{r,U}$, so as to effectively handle the nonlinear term in (1.1). In addition, \mathcal{F} itself needs to be approximated for efficiency.

Order reduction of the vector problem (1.6) is a well established procedure. Among various methods, the Proper Orthogonal Decomposition (POD) methodology has been widely employed, as it mainly relies on solution samples, rather than the a-priori generation of an appropriate basis [12],[13],[30],[37]. Other approaches include reduced basis methods, see, e.g., [44], and rational interpolation strategies [4]; see, e.g., [14] for an overview of the most common reduction strategies. The overall effectiveness of the POD procedure is largely influenced by the capability of evaluating the nonlinear term within the reduced space, motivating a considerable amount of work towards this estimation, including quadratic bilinear approximation [28, 36, 11] and trajectory piecewise-linear approximation [52]. Alternatively several approaches consider interpolating the nonlinear function, such as missing point estimation [6] and

¹Here we display the discretized Laplace operator, more general operators can be treated; see, e.g., [46, Section 3].

the best points interpolation method [42]. One very successful approach is the Discrete Empirical Interpolation Method (DEIM) [19], which is based on the Empirical Interpolation Method originally introduced in [8].

We devise a matrix-oriented POD approach tailored towards the construction of the matrix reduced problem formulation (1.4). An adaptive procedure is also developed to limit the number of snapshots contributing to the generation of the approximation spaces. The reduction of the nonlinear term is then performed by means of a fully matricial interpolation using left and right projections onto two distinct reduction spaces, giving rise to a new two-sided version of DEIM.

The idea of using left and right POD-type bases in a matrix-oriented setting is not new in the general context of semilinear differential equations (see section 4). Nonetheless, after reduction these strategies resume the vector form of (1.4) for integration purposes, thus loosing the structural and computational benefits of the matrix formulation. We claim that once (1.4) is obtained, matrix-oriented integrators should be employed. In other words, by combining matrix-oriented versions of POD, DEIM and ODE integrators, we are able to carry the whole approximation with explicit reference to the two-dimensional computational domain. As a result, a fast (offline) reduction phase where a significant decrease in the problem size is carried out, is followed by a light (online) phase where the reduced ordinary differential matrix equation is integrated over time with the preferred matrix-oriented method.

Our construction focuses on the two-dimensional problem. The advantages of our methodology become even more apparent in the three-dimensional (3D) case. A simplified version of our framework in the 3D case is experimentally explored in the companion manuscript [33], where the application to systems of differential equations is also discussed. Here we deepen the analysis of all the ingredients of this new methodology, and emphasize its advantages over the vector-based approaches with a selection of numerical results. A more extensive experimental evidence can be found in the previous version of this paper [34].

The paper is organized as follows. In section 2 we review the standard POD-DEIM algorithm for systems of the form (1.6), whereas our new two-sided proper orthogonal decomposition is derived in section 3. In section 4 we discuss the relation to other matrix-based interpolation strategies and in section 5 we present a dynamical procedure for selecting the snapshots. Section 6 is devoted to the crucial approximation of the nonlinear function by the new two-sided discrete empirical interpolation method. The overall new procedure with the numerical treatment of the reduced differential problem is summarized in section 7. Numerical experiments are reported in section 8 to illustrate the effectiveness of the proposed procedure. Technical implementation details and computational costs are discussed in Appendix A.

Notation. \mathbf{I}_n denotes the $n \times n$ identity matrix; the subscript is omitted whenever clear from the context. For a matrix \mathbf{A} , $\|\mathbf{A}\|$ denotes the matrix norm induced by the Euclidean vector norm, and $\|\mathbf{A}\|_F$ the Frobenius norm. Scalar quantities are denoted by lower case letters, while vectors (matrices) are denoted by bold face lower (capital) case letters. As an exception, matrix quantities of interest in the *vector* POD-DEIM approximation are denoted in sans-serif, instead of bold face, i.e., \mathbf{M} .

All reported experiments were performed using MATLAB 9.6 (R2020b) ([40]) on a MacBook Pro with 8-GB memory and a 2.3-GHz Intel core i5 processor.

2. The standard POD method and DEIM in the vector framework. We review the standard POD-DEIM method and its application to the dynamical system (1.6).

The proper orthogonal decomposition is a technique for reducing the dimensionality of a given dynamical system, by projecting it onto a space spanned by the orthonormal columns of a matrix \mathbf{V}_k . To this end, we consider a set of *snapshot solutions* $\mathbf{u}_j = \mathbf{u}(t_j)$ of the system (1.6) at n_s different time instances ($0 \leq t_1 < \dots < t_{n_s} \leq T_f$). Let

$$(2.1) \quad \mathbf{S} = [\mathbf{u}_1, \dots, \mathbf{u}_{n_s}] \in \mathbb{R}^{N \times n_s},$$

and $\mathcal{S} = \text{Range}(\mathbf{S})$ of dimension d . A POD basis of dimension $k < d$ is a set of orthonormal vectors whose linear span gives the best approximation, according to some criterion, of the space \mathcal{S} . In the 2-norm, this basis can be obtained through the singular value decomposition (SVD) of the matrix \mathbf{S} , $\mathbf{S} = \mathbf{V}\mathbf{\Sigma}\mathbf{W}^\top$, with \mathbf{V} and \mathbf{W} orthogonal matrices and $\mathbf{\Sigma} = \text{diag}(\sigma_1, \dots, \sigma_{n_s})$ diagonal with non-increasing positive diagonal elements. If the diagonal elements of $\mathbf{\Sigma}$ have a rapid decay, the first k columns of \mathbf{V} (left singular vectors) are the most dominant in the approximation of \mathbf{S} . Denoting with $\mathbf{S}_k = \mathbf{V}_k \mathbf{\Sigma}_k \mathbf{W}_k^\top$ the reduced SVD where only the $k \times k$ top left portion of $\mathbf{\Sigma}$ is retained and \mathbf{V}, \mathbf{W} are truncated accordingly, then $\|\mathbf{S} - \mathbf{S}_k\| = \sigma_{k+1}$ [26].

Once the matrix \mathbf{V}_k is obtained, for $t \in [0, T_f]$ the vector $\mathbf{u}(t)$ is approximated as $\mathbf{u}(t) \approx \mathbf{V}_k \mathbf{y}_k(t)$, where the vector $\mathbf{y}_k(t) \in \mathbb{R}^k$ solves the *reduced* problem

$$(2.2) \quad \dot{\mathbf{y}}_k(t) = \mathbf{L}_k \mathbf{y}_k(t) + \mathbf{f}_k(\mathbf{y}_k, t), \quad \mathbf{y}_k(0) = \mathbf{V}_k^\top \mathbf{u}_0.$$

Here $\mathbf{L}_k = \mathbf{V}_k^\top \mathbf{L} \mathbf{V}_k$ and $\mathbf{f}_k(\mathbf{y}_k, t) = \mathbf{V}_k^\top \mathbf{f}(\mathbf{V}_k \mathbf{y}_k, t)$. Although for $k \ll N$ problem (2.2) is cheaper to solve than the original one, the definition of \mathbf{f}_k above requires the evaluation of $\mathbf{f}(\mathbf{V}_k \mathbf{y}_k, t)$ at each timestep and at all N entries, thus still depending on the original system size. One way to overcome this problem is by means of DEIM.

The DEIM procedure, originally introduced in [19], is utilized to approximate a nonlinear vector function $\mathbf{f} : \mathcal{T} \rightarrow \mathbb{R}^N$ by interpolating it onto an empirical basis, that is, $\mathbf{f}(t) \approx \mathbf{\Phi}_f \mathbf{c}(t)$, where $\{\boldsymbol{\varphi}_1, \dots, \boldsymbol{\varphi}_p\} \subset \mathbb{R}^N$ is a low dimensional basis, $\mathbf{\Phi}_f = [\boldsymbol{\varphi}_1, \dots, \boldsymbol{\varphi}_p] \in \mathbb{R}^{N \times p}$ and $\mathbf{c}(t) \in \mathbb{R}^p$ is the vector of time-dependent coefficients to be determined.

Let $\mathbf{P} = [\mathbf{e}_{\rho_1}, \dots, \mathbf{e}_{\rho_p}] \in \mathbb{R}^{N \times p}$ be a subset of columns of the identity matrix, named the ‘‘selection matrix’’. If $\mathbf{P}^\top \mathbf{\Phi}_f$ is invertible, in [19] the coefficient vector $\mathbf{c}(t)$ is uniquely determined by solving the linear system $\mathbf{P}^\top \mathbf{\Phi}_f \mathbf{c}(t) = \mathbf{P}^\top \mathbf{f}(t)$, so that

$$(2.3) \quad \mathbf{f}(t) \approx \mathbf{\Phi}_f \mathbf{c}(t) = \mathbf{\Phi}_f (\mathbf{P}^\top \mathbf{\Phi}_f)^{-1} \mathbf{P}^\top \mathbf{f}(t).$$

The nonlinear term in the reduced model (2.2) is then approximated by

$$(2.4) \quad \mathbf{f}_k(\mathbf{y}_k, t) \approx \mathbf{V}_k^\top \mathbf{\Phi}_f (\mathbf{P}^\top \mathbf{\Phi}_f)^{-1} \mathbf{P}^\top \mathbf{f}(\mathbf{V}_k \mathbf{y}_k, t).$$

The accuracy of DEIM depends greatly on the basis choice, and in a lesser way by the choice of \mathbf{P} . In most applications the interpolation basis $\{\boldsymbol{\varphi}_1, \dots, \boldsymbol{\varphi}_p\}$ is selected as the POD basis of the set of snapshots $\{\mathbf{f}(\mathbf{u}_1, t_1), \dots, \mathbf{f}(\mathbf{u}_{n_s}, t_{n_s})\}$, as described earlier in this section, that is given the matrix

$$(2.5) \quad \mathbf{N} = [\mathbf{f}(\mathbf{u}_1, t_1), \dots, \mathbf{f}(\mathbf{u}_{n_s}, t_{n_s})] \in \mathbb{R}^{N \times n_s},$$

the columns of the matrix $\mathbf{\Phi}_f = [\boldsymbol{\varphi}_1, \dots, \boldsymbol{\varphi}_p]$ are determined as the first $p \leq n_s$ dominant left singular vectors in the SVD of \mathbf{N} . The matrix \mathbf{P} for DEIM is selected by a greedy algorithm based on the system residual; see [19, Algorithm 3.1]. In [23] the authors showed that a pivoted QR-factorization of $\mathbf{\Phi}_f^\top$ may lead to better accuracy

and stability properties of the computed matrix \mathbf{P} . The resulting approach, called Q-DEIM, will be used in the sequel and is implemented as algorithm `q-deim` in [23].

DEIM is particularly advantageous when the function \mathbf{f} is evaluated component-wise, in which case it holds that $\mathbf{P}^\top \mathbf{f}(\mathbf{V}_k \mathbf{y}_k, t) = \mathbf{f}(\mathbf{P}^\top \mathbf{V}_k \mathbf{y}_k, t)$, so that the nonlinear function is evaluated only at $p \ll N$ components. In general, this occurs whenever finite differences are the underlying discretization method. If more versatile discretizations are required, then different procedures need to be devised. A discussion of these approaches is deferred to section 4.

3. A new two-sided proper orthogonal decomposition. We derive a POD-DEIM algorithm that fully lives in the matrix setting, without requiring a mapping from $\mathbb{R}^{n_x \times n_y}$ to \mathbb{R}^N , so that no vectors of length N need to be processed or stored. We determine the left and right reduced space bases that approximate the space of the given snapshots $\Xi(t)$ (either the nonlinear functions or the approximate solutions), so that $\Xi(t) \approx \mathbf{V}_\ell \Theta(t) \mathbf{W}_r^\top$, where $\mathbf{V}_\ell, \mathbf{W}_r$ have ν_ℓ and ν_r orthonormal columns, respectively. Their ranges approximate the span of the rows (left) and columns (right) spaces of the function $\Xi(t)$, independently of the time t . In practice, we wish to have $\nu_\ell \ll n_x, \nu_r \ll n_y$ so that $\Theta(t)$ will have a reduced dimension. A simple way to proceed would be to collect all snapshot matrices in a single large (or tall) matrix and generate the two orthonormal bases corresponding to the rows and columns spaces. This is way too expensive, both in terms of computational costs and memory requirements. Instead, we present a two-step procedure that avoids explicit computations with all snapshots simultaneously. The first step sequentially selects the most important information of each snapshot matrix, relative to the other snapshots, while the second step prunes the generated spaces by building the corresponding orthonormal bases. These two steps can be summarized as follows:

1. *Dynamic selection.* Assume i snapshots have been processed and dominant SVD information retained. For the next snapshot $\Xi(t_{i+1})$ perform a reduced SVD and retain the leading singular triplets in a way that the retained singular values are at least as large as those already kept from previous iterations. Make sure that at most κ SVD components are retained overall, with κ selected a-priori;
2. *Bases pruning.* Ensure that the vectors spanning the reduced right and left spaces have orthonormal columns. Reduce the space dimension if needed.

In the following we provide the details for this two-step procedure. The strategy that leads to the selection of the actual time instances used for this construction will be discussed in section 5. To simplify the presentation, and without loss of generality, we assume $n_x = n_y \equiv n$.

First step. Let $\Xi_i = \Xi(t_i)$. For the collection of snapshots, we wish to determine a (left) reduced basis for the range of the matrix $\mathbf{H}\{\Xi\} := (\Xi_1, \dots, \Xi_{n_s}) \in \mathbb{R}^{n \times (n \cdot n_s)}$ and a (right) reduced basis for the range of the matrix $\mathbf{Z}\{\Xi\} = (\Xi_1^\top, \dots, \Xi_{n_s}^\top)^\top = (\Xi_1; \dots; \Xi_{n_s})$. This is performed by incrementally including leading components of the snapshots Ξ_i , so as to determine the approximations

$$\begin{aligned} \mathbf{H}\{\Xi\} &\approx \widetilde{\mathbf{H}}\{\Xi\} := \widetilde{\mathbf{V}}_{n_s} \widetilde{\Sigma}_{n_s} \widetilde{\mathbf{W}}_{n_s}^\top, & \widetilde{\mathbf{V}}_{n_s} &\in \mathbb{R}^{n \times \kappa}, \widetilde{\mathbf{W}}_{n_s} \in \mathbb{R}^{n \cdot n_s \times \kappa} \\ \mathbf{Z}\{\Xi\} &\approx \widehat{\mathbf{Z}}\{\Xi\} := \widehat{\mathbf{V}}_{n_s} \widetilde{\Sigma}_{n_s} \widehat{\mathbf{W}}_{n_s}^\top, & \widehat{\mathbf{V}}_{n_s} &\in \mathbb{R}^{n \cdot n_s \times \kappa}, \widehat{\mathbf{W}}_{n_s} \in \mathbb{R}^{n \times \kappa}. \end{aligned}$$

A rank reduction of the matrices $\widetilde{\mathbf{V}}_{n_s}$ and $\widehat{\mathbf{W}}_{n_s}$ will provide the sought after bases, to be used for time instances other than those of the snapshots. Let $\kappa \leq n$ be the chosen maximum admissible dimension for the reduced left and right spaces. For

$i \in \{1, \dots, n_s\}$, let

$$(3.1) \quad \mathbf{\Xi}_i \approx \mathbf{V}_i \mathbf{\Sigma}_i \mathbf{W}_i^\top, \quad \mathbf{V}_i, \mathbf{W}_i \in \mathbb{R}^{n \times \kappa}, \quad \mathbf{\Sigma}_i = \text{diag}(\sigma_1^{(i)}, \dots, \sigma_\kappa^{(i)})$$

be the reduced SVD of $\mathbf{\Xi}_i$ corresponding to its dominant κ singular triplets, with singular values sorted decreasingly. Let $\tilde{\mathbf{V}}_1 = \mathbf{V}_1$, $\tilde{\mathbf{\Sigma}}_1 = \mathbf{\Sigma}_1$ and $\tilde{\mathbf{W}}_1 = \mathbf{W}_1$. For each subsequent $i = 2, \dots, n_s$, the leading singular triplets of $\mathbf{\Xi}_i$ are *appended* to the previous matrices $\tilde{\mathbf{\Sigma}}_{i-1}$, $\tilde{\mathbf{V}}_{i-1}$ and $\tilde{\mathbf{W}}_{i-1}$, that is

$$(3.2) \quad \tilde{\mathbf{H}}_i\{\mathbf{\Xi}\} = (\tilde{\mathbf{V}}_{i-1}, \mathbf{V}_i) \begin{pmatrix} \tilde{\mathbf{\Sigma}}_{i-1} & \\ & \mathbf{\Sigma}_i \end{pmatrix} \begin{pmatrix} \tilde{\mathbf{W}}_{i-1}^\top & \\ & \mathbf{W}_i^\top \end{pmatrix} \equiv \tilde{\mathbf{V}}_i \tilde{\mathbf{\Sigma}}_i \tilde{\mathbf{W}}_i^\top.$$

After at most n_s iterations we will have the final $\tilde{\mathbf{H}}\{\mathbf{\Xi}\}$, with no subscript. The expansion is performed ensuring that the appended singular values are at least as large as those already present, so that the retained directions are the leading ones among all snapshots. Then the three matrices $\tilde{\mathbf{V}}_i$, $\tilde{\mathbf{W}}_i$ and $\tilde{\mathbf{\Sigma}}_i$ are truncated so that the retained diagonal entries of $\tilde{\mathbf{\Sigma}}_i$ are its κ largest diagonal elements. The diagonal elements of $\tilde{\mathbf{\Sigma}}_i$ are not the singular values of $\mathbf{H}_i\{\mathbf{\Xi}\}$, however the adopted truncation strategy ensures that the error committed is not larger than $\sigma_{\kappa+1}$, which we define as the largest singular value discarded during the whole accumulation process. Since each column of $\tilde{\mathbf{V}}_{n_s}$ has unit norm, it follows that $\|\tilde{\mathbf{V}}_{n_s}\| \leq \kappa$. Moreover, the columns of $\tilde{\mathbf{W}}_{n_s}$ are orthonormal. Hence $\|\mathbf{H}\{\mathbf{\Xi}\} - \tilde{\mathbf{H}}\{\mathbf{\Xi}\}\| \leq \kappa \sigma_{\kappa+1}$. In particular, this procedure is not the same as taking the leading singular triplets of each snapshot *when compared with all snapshots*, using the magnitude of all singular values as quality measure.

A similar strategy is adopted to construct the right basis. Formally,

$$(3.3) \quad \hat{\mathbf{Z}}_i\{\mathbf{\Xi}\} = \begin{pmatrix} \hat{\mathbf{V}}_{i-1} & \\ & \mathbf{V}_i \end{pmatrix} \begin{pmatrix} \tilde{\mathbf{\Sigma}}_{i-1} & \\ & \mathbf{\Sigma}_i \end{pmatrix} \begin{pmatrix} \hat{\mathbf{W}}_{i-1}^\top & \\ & \mathbf{W}_i^\top \end{pmatrix} = \hat{\mathbf{V}}_i \tilde{\mathbf{\Sigma}}_i \hat{\mathbf{W}}_i^\top;$$

notice that $\tilde{\mathbf{\Sigma}}_i$ is the same for both $\tilde{\mathbf{H}}$ and $\hat{\mathbf{Z}}$, and that the large matrices $\tilde{\mathbf{W}}_i$ and $\hat{\mathbf{V}}_i$ are not stored explicitly in the actual implementation. At completion, the following two matrices are bases candidates for the left and right spaces:

$$(3.4) \quad \text{Left : } \tilde{\mathbf{V}}_{n_s} \tilde{\mathbf{\Sigma}}_{n_s}^{\frac{1}{2}}, \quad \text{Right : } \tilde{\mathbf{\Sigma}}_{n_s}^{\frac{1}{2}} \hat{\mathbf{W}}_{n_s}^\top,$$

where the singular value matrices keep track of the relevance of each collected singular vector, and the square root allows us to maintain the order of magnitude of the snapshot matrices, when the product of the two left and right matrices is carried out. Here n_s is the total number of snapshots included in the whole procedure, using the dynamic procedure discussed in section 5.

The procedure is described in Algorithm 3.1.

Second step. We complete the two-sided approximation of the snapshot functions by pruning the two orthonormal bases associated with the representation (3.4). Let

$$(3.5) \quad \tilde{\mathbf{V}}_{n_s} \tilde{\mathbf{\Sigma}}_{n_s}^{\frac{1}{2}} = \overline{\mathbf{V}} \overline{\mathbf{\Sigma}} \overline{\mathbf{W}}^\top \quad \text{and} \quad \tilde{\mathbf{\Sigma}}_{n_s}^{\frac{1}{2}} \hat{\mathbf{W}}_{n_s}^\top = \check{\mathbf{V}} \check{\mathbf{\Sigma}} \check{\mathbf{W}}^\top$$

be the singular value decompositions of the given matrices. If the matrices $\overline{\mathbf{\Sigma}}$ and $\check{\mathbf{\Sigma}}$

Algorithm 3.1 DYNAMIC SELECTION PROCEDURE

- 1: **INPUT:** $\Xi_i, \tilde{\mathbf{V}}_{i-1} \in \mathbb{R}^{n \times \kappa}, \tilde{\Sigma}_{i-1} \in \mathbb{R}^{\kappa \times \kappa}, \widehat{\mathbf{W}}_{i-1} \in \mathbb{R}^{n \times \kappa}, \kappa$
 - 2: **OUTPUT:** $\tilde{\mathbf{V}}_i \in \mathbb{R}^{n \times \kappa}, \tilde{\Sigma}_i \in \mathbb{R}^{\kappa \times \kappa}, \widehat{\mathbf{W}}_i \in \mathbb{R}^{n \times \kappa}$.
 - 3: Compute $[\mathbf{V}_i, \Sigma_i, \mathbf{W}_i] = \text{svds}(\Xi_i, \kappa)$;
 - 4: Append $\tilde{\mathbf{V}}_i \leftarrow (\tilde{\mathbf{V}}_{i-1}, \mathbf{V}_i), \widehat{\mathbf{W}}_i \leftarrow (\widehat{\mathbf{W}}_{i-1}, \mathbf{W}_i), \tilde{\Sigma}_i \leftarrow \text{blkdiag}(\tilde{\Sigma}_{i-1}, \Sigma_i)$;
 - 5: Decreasingly order the entries of (diagonal) $\tilde{\Sigma}_i$ and keep the first κ ;
 - 6: Order $\tilde{\mathbf{V}}_i$ and $\widehat{\mathbf{W}}_i$ accordingly and keep the first κ vectors of each;
-

have rapidly decaying singular values, we can further reduce the low rank approximation of each Ξ_i . More precisely, let

$$(3.6) \quad \bar{\mathbf{V}} \bar{\Sigma} = [\mathbf{V}_\ell, \mathbf{V}_\mathcal{E}] \begin{pmatrix} \bar{\Sigma}_\ell & \\ & \bar{\Sigma}_\mathcal{E} \end{pmatrix}, \quad \text{and} \quad \check{\Sigma} \check{\mathbf{W}}^\top = \begin{pmatrix} \check{\Sigma}_r & \\ & \check{\Sigma}_\mathcal{E} \end{pmatrix} \begin{bmatrix} \mathbf{W}_r^\top \\ \mathbf{W}_\mathcal{E}^\top \end{bmatrix},$$

with $\mathbf{V}_\ell \in \mathbb{R}^{n \times \nu_\ell}, \mathbf{W}_r \in \mathbb{R}^{n \times \nu_r}$. The final reduced dimensions ν_ℓ and ν_r , that is the number of columns to be retained in the matrices \mathbf{V}_ℓ and \mathbf{W}_r , respectively, is determined by the following criterion:

$$(3.7) \quad \|\bar{\Sigma}_\mathcal{E}\|_F \leq \frac{\tau}{\sqrt{n_{\max}}} \|\bar{\Sigma}\|_F \quad \text{and} \quad \|\check{\Sigma}_\mathcal{E}\|_F \leq \frac{\tau}{\sqrt{n_{\max}}} \|\check{\Sigma}\|_F,$$

for some chosen tolerance $\tau \in (0, 1)$ and n_{\max} is the maximum number of available snapshots of the considered function.

We have assumed so far that at least one singular triplet is retained for all Ξ 's. In practice, it might happen that for some i none of the singular values is large enough to be retained. In this case, Ξ_i does not contribute to the two-sided basis.

REMARK 3.1. *If $\Xi_i = \Xi(t_i)$ is symmetric for $t_i \in [0, T_f]$, the reduction process can preserve this structure. Indeed, since Ξ_i is symmetric it holds that $\Xi_i = \mathbf{V}_i \Sigma_i \mathbf{W}_i^\top = \mathbf{V}_i \Sigma_i \mathbf{D}_i \mathbf{V}_i^\top$, with \mathbf{D}_i diagonal of ones and minus ones. As a consequence, $\mathbf{W}_r = \mathbf{V}_\ell$. Positive definiteness can also be preserved, with \mathbf{D}_i the identity matrix.*

In the following we use the pair $(\mathbf{V}_\ell, \mathbf{W}_r)$, hereafter denoted as *two-sided proper orthogonal decomposition* (2S-POD), to approximate the function $\Xi(t)$ for some $t \neq t_i$:

$$(3.8) \quad \Xi(t) \approx \mathbf{V}_{\ell, \Xi} \Theta(t) \mathbf{W}_{r, \Xi}^\top$$

with Θ depending on t , of reduced dimension, and $\mathbf{V}_{\ell, \Xi}$ and $\mathbf{W}_{r, \Xi}$ play the role of \mathbf{V}_ℓ and \mathbf{W}_r respectively.

4. Connections to other matrix-based interpolation POD strategies.

The approximation discussed in the previous section is not restricted to problems of the form (1.1), but rather it can be employed to any POD function approximation where the snapshot vectors are transformed into matrices, giving rise to a matrix DEIM methodology. This class of approximation has been explored in the recent literature, where different approaches have been discussed, especially in connection with parameter-dependent problems and Jacobian matrix approximation; see, e.g., [53],[18], and the thorough discussion in [12]. In the former case, the setting is particularly appealing whenever the operator has a parameter-based affine function formulation, while in the Jacobian case the problem is naturally stated in matrix terms, possibly with a sparse structure [15],[49]. In the nonaffine case, in [15],[41] an affine

matrix approximation (MDEIM) was proposed by writing appropriate (local) sparse representations of the POD basis, as is the case for finite element methods. As an alternative in this context, it was shown in [22] that DEIM can be applied locally to functions defined on the unassembled finite element mesh (UDEIM); we refer the reader to [50] for more details and to [3] for a detailed experimental analysis.

In our approach we consider the approximation in (3.8). If $\Theta(t)$ were diagonal, then this approximation could be thought of as an MDEIM approach, since then $\Xi(t)$ would be approximated by a sum of rank-one matrices with the time-dependent diagonal elements of $\Theta(t)$ as coefficients. Instead, in our setting $\Theta(t)$ is far from diagonal, hence our approximation determines a more general memory saving approximation based on the low rank representation given by $\mathbf{V}_{\ell,\Xi}, \mathbf{W}_{r,\Xi}$.

Another crucial novel fact of our approach is the following. While methods such as MDEIM aim at creating a linear combination of matrices, they still rely on the vector DEIM for computing these matrices, thus only detecting the leading portion of the left range space. In our construction, the left and right approximation spaces spanned by $\mathbf{V}_{\ell,\Xi}, \mathbf{W}_{r,\Xi}$, respectively, stem from a subspace selection of the range spaces of the whole snapshot matrix $\mathbf{H}\{\Xi\}$ (left space) and $\mathbf{Z}\{\Xi\}$ (right space); here both spaces are *matrix* spaces. In this way, the leading components of both spaces can be captured. In particular, specific space directions taken by the approximated function during the time evolution can be more easily tracked; we refer to the previous version of this manuscript for an experimental illustration [34, section 8.1].

In light of the discussion above, our approach might also be interpreted in terms of the ‘‘local basis’’ POD framework, see, e.g., [2], where the generality of the bases is ensured by interpolation onto matrix manifolds. For a presentation of this methodology we also refer the reader to the insightful survey [12, section 4.2]. In this context, the matrices $\mathbf{V}_{\ell}, \mathbf{W}_r$ may represent a new *truncated* interpolation of the matrices in $\mathbf{H}\{\Xi\}$ and $\mathbf{Z}\{\Xi\}$, in a completely algebraic setting.

5. A dynamic algorithm for creating the 2S-POD approximation space.

We describe an adaptive procedure for selecting the time instances employed in the first step of the basis construction of section 3. This procedure will be used for the selection of both the solution and the nonlinear function snapshots. The dynamic procedure starts with a coarse discretization of the time interval (using one fourth of the available nodes), and then continues with two successive refinements if needed.

Let n_{\max} be the maximum number of available snapshots of the considered function $\Xi(t)$, $t \in [t_0, T_f]$ with $t_0 = 0$. A first set \mathcal{I}_1 of $n_{\max}/4$ equispaced time instances in $[0, T_f]$ is considered (symbol ‘ \star ’ in Figure 5.1). If needed, a second set \mathcal{I}_2 of $n_{\max}/4$ equispaced time instances are considered (symbol ‘ \times ’), whereas the remaining $n_{\max}/2$ time instances (symbol ‘ \square ’ and set \mathcal{I}_3) are considered in the third phase, if needed at all.

The initial 2S-POD basis matrices of dimension κ , i.e. $\tilde{\mathbf{V}}_1$ and $\widehat{\mathbf{W}}_1$ from (3.4), are constructed by processing the snapshot $\Xi(t_0)$. For all other time instances t_i in each phase, we use the following inclusion criterion

$$(5.1) \quad \text{if } \epsilon_i := \frac{\|\Xi(t_i) - \Pi_{\ell}\Xi(t_i)\Pi_r\|}{\|\Xi(t_i)\|} > \text{tol} \quad \text{then include}$$

where Π_{ℓ} and Π_r are orthogonal projectors onto the left and right spaces (these are implicitly constructed by performing a reduced QR decomposition of the current matrices $\tilde{\mathbf{V}}_i$ and $\widehat{\mathbf{W}}_i$ on the fly). If a snapshot is selected for inclusion, the leading singular triplets of $\Xi(t_i)$ are appended to the current bases, and the leading κ components are

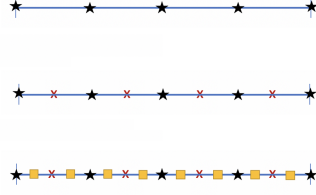


Fig. 5.1: The three evaluation phases of the refinement procedure.

retained as in Algorithm 3.1; then the next time instance in the phase is investigated. If, by the end of the phase, the arithmetic mean of the errors ϵ_i in (5.1) is above tol , it means that the bases are not sufficiently good and we move on to the next refinement phase. Otherwise, the snapshot selection procedure is ended and the matrices $\bar{\mathbf{V}}$ and $\bar{\mathbf{W}}$ are computed and pruned by the second step in section 3 to form the final 2S-POD basis matrices $\mathbf{V}_{\ell, \Xi} \in \mathbb{R}^{n \times \nu_\ell}$ and $\mathbf{W}_{r, \Xi} \in \mathbb{R}^{n \times \nu_r}$. The full DYNAMIC procedure to create the 2S-POD approximation space is presented in Algorithm 5.1.

Algorithm 5.1 DYNAMIC 2S-POD

- 1: **INPUT:** Function $\Xi : \mathcal{T} \mapsto \mathbb{R}^{n \times n}$, n_{\max} , tol , κ , phase sets $\mathcal{I}_{1,2,3}$
 - 2: **OUTPUT:** $\mathbf{V}_{\ell, \Xi} \in \mathbb{R}^{n \times \nu_\ell}$ and $\mathbf{W}_{r, \Xi} \in \mathbb{R}^{n \times \nu_r}$
 - 3: Compute $[\mathbf{V}_1, \Sigma_1, \mathbf{W}_1] = \text{svds}(\Xi(t_0), \kappa)$;
 - 4: Let $\tilde{\mathbf{V}}_1 = \mathbf{V}_1$, $\tilde{\mathbf{W}}_1 = \mathbf{W}_1$, $\tilde{\Sigma}_1 = \Sigma_1$;
 - 5: *Dynamic selection step :*
 - 6: **for** PHASE = 1, 2, 3 **do**
 - 7: **for all** $t_i \in \mathcal{I}_{\text{PHASE}}$ **do**
 - 8: **if** (5.1) satisfied **then**
 - 9: Process snapshot $\Xi(t_i)$ using Dynamic selection (Algorithm 3.1);
 - 10: Update $\tilde{\mathbf{V}}_i$ and $\tilde{\mathbf{W}}_i$;
 - 11: **end if**
 - 12: **end for**
 - 13: **if** $\sum_{t_i \in \mathcal{I}_{\text{PHASE}}} \epsilon_i \leq \text{tol} |\mathcal{I}_{\text{PHASE}}|$ **then**
 - 14: **break** and go to 17;
 - 15: **end if**
 - 16: **end for**
 - 17: *Bases Pruning:*
 - 18: Determine the reduced SVD of $\tilde{\mathbf{V}}_{n_s} \tilde{\Sigma}_{n_s}^{\frac{1}{2}}$ and $\tilde{\Sigma}_{n_s}^{\frac{1}{2}} \tilde{\mathbf{W}}_{n_s}^\top$ in (3.5);
 - 19: Determine the final reduced $\mathbf{V}_{\ell, \Xi}$ and $\mathbf{W}_{r, \Xi}$ as in (3.6) using the criterion (3.7);
 - 20: **Stop**
-

6. Approximation of the nonlinear function \mathcal{F}_k in the reduced model.

To complete the reduction of the original problem to the small size problem (1.4), we need to discuss the derivation of the approximation $\widehat{\mathcal{F}_k(\mathbf{Y}_k, t)}$. Let $\{\mathcal{F}(t_j)\}_{j=1}^{n_s}$ be a set of snapshots of the nonlinear function \mathcal{F} at times t_j , $j = 1, \dots, n_s$. Using Algorithm 5.1 we compute the two matrices $\mathbf{V}_{\ell, \mathcal{F}} \in \mathbb{R}^{n \times p_1}$, $\mathbf{W}_{r, \mathcal{F}} \in \mathbb{R}^{n \times p_2}$ so as to

approximate $\mathcal{F}(t)$ as

$$(6.1) \quad \mathcal{F}(t) \approx \mathbf{V}_{\ell, \mathcal{F}} \mathbf{C}(t) \mathbf{W}_{r, \mathcal{F}}^\top,$$

with $\mathbf{C}(t)$ to be determined. Here p_1, p_2 play the role of ν_ℓ, ν_r in the general description, and they will be used throughout as basis truncation parameters for the nonlinear snapshots. By adapting the DEIM idea to a two-sided perspective, the coefficient matrix $\mathbf{C}(t)$ is determined by selecting independent rows from the matrices $\mathbf{V}_{\ell, \mathcal{F}}$ and $\mathbf{W}_{r, \mathcal{F}}$, so that

$$\mathbf{P}_{\ell, \mathcal{F}}^\top \mathbf{V}_{\ell, \mathcal{F}} \mathbf{C}(t) \mathbf{W}_{r, \mathcal{F}}^\top \mathbf{P}_{r, \mathcal{F}} = \mathbf{P}_{\ell, \mathcal{F}}^\top \mathcal{F}(t) \mathbf{P}_{r, \mathcal{F}},$$

where $\mathbf{P}_{\ell, \mathcal{F}} = [e_{\pi_1}, \dots, e_{\pi_{p_1}}] \in \mathbb{R}^{n \times p_1}$ and $\mathbf{P}_{r, \mathcal{F}} = [e_{\gamma_1}, \dots, e_{\gamma_{p_2}}] \in \mathbb{R}^{n \times p_2}$ are columns of the identity matrix of size n . Both matrices are defined similarly to the selection matrix \mathbf{P} from section 2, and they act on $\mathbf{V}_{\ell, \mathcal{F}}, \mathbf{W}_{r, \mathcal{F}}$, respectively. If $\mathbf{P}_{\ell, \mathcal{F}}^\top \mathbf{V}_{\ell, \mathcal{F}}$ and $\mathbf{P}_{r, \mathcal{F}}^\top \mathbf{W}_{r, \mathcal{F}}$ are nonsingular, then the coefficient matrix $\mathbf{C}(t)$ is determined by

$$\mathbf{C}(t) = (\mathbf{P}_{\ell, \mathcal{F}}^\top \mathbf{V}_{\ell, \mathcal{F}})^{-1} \mathbf{P}_{\ell, \mathcal{F}}^\top \mathcal{F}(t) \mathbf{P}_{r, \mathcal{F}} (\mathbf{W}_{r, \mathcal{F}}^\top \mathbf{P}_{r, \mathcal{F}})^{-1}.$$

With this coefficient matrix $\mathbf{C}(t)$, the final approximation (6.1) becomes²

$$(6.2) \quad \tilde{\mathcal{F}}(t) = \mathbf{V}_{\ell, \mathcal{F}} (\mathbf{P}_{\ell, \mathcal{F}}^\top \mathbf{V}_{\ell, \mathcal{F}})^{-1} \mathbf{P}_{\ell, \mathcal{F}}^\top \mathcal{F}(t) \mathbf{P}_{r, \mathcal{F}} (\mathbf{W}_{r, \mathcal{F}}^\top \mathbf{P}_{r, \mathcal{F}})^{-1} \mathbf{W}_{r, \mathcal{F}}^\top =: \mathbf{Q}_{\ell, \mathcal{F}} \mathcal{F}(t) \mathbf{Q}_{r, \mathcal{F}}^\top.$$

Note that $\mathbf{Q}_{*, \mathcal{F}}$ are oblique projectors. A similar approximation can be found in [48]. In addition to that of the two spaces, an important role is played by the choice of the interpolation indices contained in $\mathbf{P}_{\ell, \mathcal{F}}$ and $\mathbf{P}_{r, \mathcal{F}}$. We suggest determining these indices for the matrices $\mathbf{P}_{\ell, \mathcal{F}}$ and $\mathbf{P}_{r, \mathcal{F}}$ as the output of `q-deim` ([23]) with inputs $\mathbf{V}_{\ell, \mathcal{F}}$ and $\mathbf{W}_{r, \mathcal{F}}$, respectively.

We next provide a bound measuring the distance between the error obtained with the proposed oblique projection (6.2) and the best approximation error of \mathcal{F} in the same range spaces, where we recall that $\mathbf{V}_{\ell, \mathcal{F}}$ and $\mathbf{W}_{r, \mathcal{F}}$ have orthonormal columns. This bound is a direct extension to the matrix setting of [19, Lemma 3.2].

PROPOSITION 6.1. *Let $\mathcal{F} \in \mathbb{R}^{n \times n}$ be an arbitrary matrix, and let $\tilde{\mathcal{F}} = \mathbf{Q}_{\ell, \mathcal{F}} \mathcal{F} \mathbf{Q}_{r, \mathcal{F}}^\top$, as in (6.2). Then*

$$(6.3) \quad \|\mathcal{F} - \tilde{\mathcal{F}}\|_F \leq c_\ell c_r \|\mathcal{F} - \mathbf{V}_{\ell, \mathcal{F}} \mathbf{V}_{\ell, \mathcal{F}}^\top \mathcal{F} \mathbf{W}_{r, \mathcal{F}} \mathbf{W}_{r, \mathcal{F}}^\top\|_F$$

where $c_\ell = \left\| (\mathbf{P}_{\ell, \mathcal{F}}^\top \mathbf{V}_{\ell, \mathcal{F}})^{-1} \right\|_2$ and $c_r = \left\| (\mathbf{P}_{r, \mathcal{F}}^\top \mathbf{W}_{r, \mathcal{F}})^{-1} \right\|_2$.

Proof. Recall that $\mathbf{f} = \text{vec}(\mathcal{F})$. Then, by the properties of the Kronecker product

$$\begin{aligned} \|\mathcal{F} - \tilde{\mathcal{F}}\|_F &= \|\text{vec}(\mathcal{F}) - \text{vec}(\tilde{\mathcal{F}})\|_2 = \|\mathbf{f} - (\mathbf{Q}_{r, \mathcal{F}} \otimes \mathbf{Q}_{\ell, \mathcal{F}}) \mathbf{f}\|_2 \\ &= \left\| \mathbf{f} - (\mathbf{W}_{r, \mathcal{F}} \otimes \mathbf{V}_{\ell, \mathcal{F}}) \left((\mathbf{P}_{r, \mathcal{F}} \otimes \mathbf{P}_{\ell, \mathcal{F}})^\top (\mathbf{W}_{r, \mathcal{F}} \otimes \mathbf{V}_{\ell, \mathcal{F}}) \right)^{-1} (\mathbf{P}_{r, \mathcal{F}} \otimes \mathbf{P}_{\ell, \mathcal{F}})^\top \mathbf{f} \right\|_2 \end{aligned}$$

Therefore, by [19, Lemma 3.2],

$$\begin{aligned} \|\mathcal{F} - \tilde{\mathcal{F}}\|_F &\leq \left\| \left((\mathbf{P}_{r, \mathcal{F}} \otimes \mathbf{P}_{\ell, \mathcal{F}})^\top (\mathbf{W}_{r, \mathcal{F}} \otimes \mathbf{V}_{\ell, \mathcal{F}}) \right)^{-1} \right\|_2 \left\| \mathbf{f} - (\mathbf{W}_{r, \mathcal{F}} \otimes \mathbf{V}_{\ell, \mathcal{F}}) (\mathbf{W}_{r, \mathcal{F}} \otimes \mathbf{V}_{\ell, \mathcal{F}})^\top \mathbf{f} \right\|_2 \\ &= \left\| (\mathbf{P}_{\ell, \mathcal{F}}^\top \mathbf{V}_{\ell, \mathcal{F}})^{-1} \right\|_2 \left\| (\mathbf{P}_{r, \mathcal{F}}^\top \mathbf{W}_{r, \mathcal{F}})^{-1} \right\|_2 \left\| \mathcal{F} - \mathbf{V}_{\ell, \mathcal{F}} \mathbf{V}_{\ell, \mathcal{F}}^\top \mathcal{F} \mathbf{W}_{r, \mathcal{F}} \mathbf{W}_{r, \mathcal{F}}^\top \right\|_F. \quad \square \end{aligned}$$

²If the nonlinear function $\mathcal{F}(t)$ is symmetric for all $t \in [0, T_f]$, thanks to Remark 3.1 this approximation will preserve the symmetry of the nonlinear function.

We emphasize that c_ℓ, c_r do not depend on time, in case \mathcal{F} does. As has been discussed in [19],[23], it is clear from (6.3) that minimizing these amplification factors will minimize the error norm with respect to the best approximation onto the spaces $\text{Range}(\mathbf{V}_{\ell,\mathcal{F}})$ and $\text{Range}(\mathbf{W}_{r,\mathcal{F}})$. The quantities c_ℓ, c_r depend on the interpolation indices. If the indices are selected greedily, as in [19], then

$$(6.4) \quad c_\ell \leq \frac{(1 + \sqrt{2n})^{p_1 - 1}}{\|e_1^T \mathbf{V}_{\ell,\mathcal{F}}\|_\infty}, \quad c_r \leq \frac{(1 + \sqrt{2n})^{p_2 - 1}}{\|e_1^T \mathbf{W}_{r,\mathcal{F}}\|_\infty}.$$

If the indices are selected by a pivoted QR factorization as in `q-deim`, then

$$c_\ell \leq \sqrt{n - p_1 + 1} \frac{\sqrt{4^{p_1} + 6p_1 - 1}}{3}, \quad c_r \leq \sqrt{n - p_2 + 1} \frac{\sqrt{4^{p_2} + 6p_2 - 1}}{3},$$

which are better bounds than those in (6.4), though still rather pessimistic; see [23].

To complete the efficient derivation of the reduced model in (1.4) we are left with the final approximation of \mathcal{F}_k in (6.2). If \mathcal{F} is evaluated componentwise, as we assume throughout³, then $\mathbf{P}_{\ell,\mathcal{F}}^\top \mathcal{F}(\mathbf{V}_{\ell,U} \mathbf{Y}(t) \mathbf{W}_{r,U}^\top, t) \mathbf{P}_{r,\mathcal{F}} = \mathcal{F}(\mathbf{P}_{\ell,\mathcal{F}}^\top \mathbf{V}_{\ell,U} \mathbf{Y}(t) \mathbf{W}_{r,U}^\top \mathbf{P}_{r,\mathcal{F}}, t)$, so that

$$(6.5) \quad \begin{aligned} \mathcal{F}_k(\mathbf{Y}_k, t) &\approx \mathbf{V}_{\ell,U}^\top \mathbf{V}_{\ell,\mathcal{F}} (\mathbf{P}_{\ell,\mathcal{F}}^\top \mathbf{V}_{\ell,\mathcal{F}})^{-1} \mathbf{P}_{\ell,\mathcal{F}}^\top \mathcal{F}(\mathbf{V}_{\ell,U} \mathbf{Y}_k(t) \mathbf{W}_{r,U}^\top, t) \mathbf{P}_{r,\mathcal{F}} (\mathbf{W}_{r,\mathcal{F}}^\top \mathbf{P}_{r,\mathcal{F}})^{-1} \mathbf{W}_{r,\mathcal{F}}^\top \mathbf{W}_{r,U} \\ &= \mathbf{V}_{\ell,U}^\top \mathbf{V}_{\ell,\mathcal{F}} (\mathbf{P}_{\ell,\mathcal{F}}^\top \mathbf{V}_{\ell,\mathcal{F}})^{-1} \mathcal{F}(\mathbf{P}_{\ell,\mathcal{F}}^\top \mathbf{V}_{\ell,U} \mathbf{Y}_k(t) \mathbf{W}_{r,U}^\top \mathbf{P}_{r,\mathcal{F}}, t) (\mathbf{W}_{r,\mathcal{F}}^\top \mathbf{P}_{r,\mathcal{F}})^{-1} \mathbf{W}_{r,\mathcal{F}}^\top \mathbf{W}_{r,U} \\ &=: \overline{\mathcal{F}_k(\mathbf{Y}_k, t)}. \end{aligned}$$

The matrices $\mathbf{V}_{\ell,U}^\top \mathbf{V}_{\ell,\mathcal{F}} (\mathbf{P}_{\ell,\mathcal{F}}^\top \mathbf{V}_{\ell,\mathcal{F}})^{-1} \in \mathbb{R}^{k_1 \times p_1}$ and $(\mathbf{W}_{r,\mathcal{F}}^\top \mathbf{P}_{r,\mathcal{F}})^{-1} \mathbf{W}_{r,\mathcal{F}}^\top \mathbf{W}_{r,U} \in \mathbb{R}^{p_2 \times k_2}$ are independent of t , therefore they can be precomputed and stored once for all. Similarly for the products $\mathbf{P}_{\ell,\mathcal{F}}^\top \mathbf{V}_{\ell,U} \in \mathbb{R}^{p_1 \times k_1}$ and $\mathbf{W}_{r,U}^\top \mathbf{P}_{r,\mathcal{F}} \in \mathbb{R}^{k_2 \times p_2}$. Note that products involving the selection matrices \mathbf{P} 's are not explicitly carried out: the operation simply requires selecting corresponding rows or columns in the other matrix factor.

Finally, we remark that in some cases the full space approximation matrix may not be involved. For instance, if \mathcal{F} is a matrix function ([29]) and $\mathbf{U}(t)$ is symmetric for all $t \in [0, T_f]$, so that $\mathbf{U}(t) \approx \mathbf{V}_{\ell,U} \mathbf{Y}_k(t) \mathbf{V}_{\ell,U}^\top$, then, recalling (1.5), it holds that

$$\mathcal{F}_k(\mathbf{Y}_k, t) = \mathbf{V}_{\ell,U}^\top \mathcal{F}(\mathbf{V}_{\ell,U} \mathbf{Y}_k \mathbf{V}_{\ell,U}^\top, t) \mathbf{V}_{\ell,U} \stackrel{*}{=} \mathcal{F}(\mathbf{V}_{\ell,U}^\top \mathbf{V}_{\ell,U} \mathbf{Y}_k, t) = \mathcal{F}(\mathbf{Y}_k, t),$$

where the equality $\stackrel{*}{=}$ is due to [29, Corollary 1.34].

7. Two-sided POD-DEIM for nonlinear matrix-valued ODEs. To complete the derivation of the numerical method, we need to determine the time-dependent matrix $\mathbf{Y}_k(t)$, $t \in [0, T_f]$ in the approximation $\mathbf{V}_{\ell,U} \mathbf{Y}_k(t) \mathbf{W}_{r,U}^\top \approx \mathbf{U}(t)$, where $\mathbf{V}_{\ell,U} \in \mathbb{R}^{n \times k_1}$ and $\mathbf{W}_{r,U} \in \mathbb{R}^{n \times k_2}$, $k_1, k_2 \ll n$ and we let $k = (k_1, k_2)$. The function $\mathbf{Y}_k(t)$ is computed as the numerical solution to the reduced problem (1.4) with $\overline{\mathcal{F}_k(\mathbf{Y}_k, t)}$ defined in (6.5). To integrate the reduced order model (1.4) as time t varies, several alternatives can be considered. The vectorized form of the semilinear problem can be treated with classical first or second order semi-implicit methods such as IMEX

³For general nonlinear functions the theory from [19, Section 3.5] can be extended to both matrices $\mathbf{V}_{\ell,U}$ and $\mathbf{W}_{r,U}$.

methods (see, e.g., [5]), that appropriately handle the stiff and non-stiff parts of the equation. Several of these methods were originally constructed as rational approximations to exponential integrators, which have for long time been regarded as too expensive for practical purposes. Recent advances in numerical linear algebra have allowed a renewed interest in these powerful methods, see, e.g., [16, 25, 27]. One of the advantages of our matrix setting is that exponential integrators can be far more cheaply applied than in the vector case, thus allowing for a better treatment of the stiff component in the solution; see, e.g., [21]. Let $\{t_i\}_{i=0, \dots, n_t}$ be the nodes discretizing the time interval $[0, T_f]$ with meshsize h . Given the (vector) differential equation $\dot{\mathbf{y}} = \mathbf{L}_k \mathbf{y} + f(t, \mathbf{y})$, the (first order) exponential time differencing (ETD) Euler method is given by the following recurrence,

$$\mathbf{y}^{(i)} = e^{h\mathbf{L}_k} \mathbf{y}^{(i-1)} + h\varphi_1(h\mathbf{L}_k) f(t_{i-1}, \mathbf{y}^{(i-1)}),$$

where $\varphi_1(z) = (e^z - 1)/z$. In our setting, $\mathbf{L}_k = \mathbf{B}_k^\top \otimes \mathbf{I}_{k_1} + \mathbf{I}_{k_2} \otimes \mathbf{A}_k$, for which it holds that $e^{h\mathbf{L}_k} = e^{h\mathbf{B}_k^\top} \otimes e^{h\mathbf{A}_k}$ [29, Th.10.9], so that the computation of the exponential of the large matrix \mathbf{L}_k reduces to $e^{h\mathbf{L}_k} \mathbf{vec}(\mathbf{Y}_k) = \mathbf{vec}(e^{h\mathbf{A}_k} \mathbf{Y}_k e^{h\mathbf{B}_k})$. The two matrices used in the exponential functions have now small dimensions, so that the computation of the matrix exponential is fully affordable. As a consequence, the integration step can be performed all at the matrix level, without resorting to the vectorized form. More precisely (see also [21]), let $\mathfrak{f}(\mathbf{Y}_k^{(i-1)}) = \mathcal{F}_k(\mathbf{Y}_k^{(i-1)}, t_{i-1})$. Then we can compute $\mathbf{Y}_k^{(i)} \approx \mathbf{Y}_k(t_i)$ as

$$\mathbf{Y}_k^{(i)} = e^{h\mathbf{A}_k} \mathbf{Y}_k^{(i-1)} e^{h\mathbf{B}_k} + h\mathbf{\Phi}^{(i-1)},$$

where the matrix $\mathbf{\Phi}^{(i-1)}$ solves the following linear (Sylvester) matrix equation

$$(7.1) \quad \mathbf{A}_k \mathbf{\Phi} + \mathbf{\Phi} \mathbf{B}_k = e^{h\mathbf{A}_k} \mathfrak{f}(\mathbf{Y}_k^{(i-1)}) e^{h\mathbf{B}_k} - \mathfrak{f}(\mathbf{Y}_k^{(i-1)}).$$

At each iteration, the application of the matrix exponentials in \mathbf{A}_k and \mathbf{B}_k is required, together with the solution of the small dimensional Sylvester equation. This linear equation has a unique solution if and only if the spectra of \mathbf{A}_k and $-\mathbf{B}_k$ are disjoint, a hypothesis that is satisfied in our setting. The solution $\mathbf{\Phi}^{(i-1)}$ can be obtained by using the Bartels-Stewart method [9]. In case of symmetric \mathbf{A}_k and \mathbf{B}_k , significant computational savings can be obtained by computing the eigendecomposition of these two matrices at the beginning of the online phase, and then compute both the exponential and the solution to the Sylvester equation explicitly; we refer the reader to [21] for these implementation details. Matrix-oriented first order IMEX schemes could also be employed (see [21]), however in our experiments ETD provided smaller errors at comparable computational costs.

Concerning the quality of our approximation, error estimates for the full POD-DEIM approximation of systems of the form (1.6) have been derived in [53, 20], which also take into account the error incurred in the numerical solution of the reduced problem. A crucial hypothesis in the available literature is that $\mathbf{f}(\mathbf{u}, t) = \mathbf{vec}(\mathcal{F}(\mathbf{U}, t))$ be Lipschitz continuous with respect to the first argument, and this is also required for exponential integrators. This condition is satisfied for the nonlinear function of our reduced problem. Indeed, consider the vectorized approximation space $\mathbb{V}_{\mathbf{u}} = \mathbf{W}_{r, \mathbf{U}} \otimes \mathbf{V}_{\ell, \mathbf{U}}$ and the oblique projector $\mathbb{Q}_{\mathbf{f}} = \mathbf{Q}_{r, \mathcal{F}} \otimes \mathbf{Q}_{\ell, \mathcal{F}}$ from (6.2). If we denote by $\hat{\mathbf{Y}}_k(t)$ the approximate solution of (1.4) with \mathcal{F}_k approximated above, then

$$(7.2) \quad \|\mathbf{U}(t) - \mathbf{V}_{\ell, \mathbf{U}} \hat{\mathbf{Y}}_k(t) \mathbf{W}_{r, \mathbf{U}}^\top\|_F = \|\mathbf{u}(t) - \mathbb{V}_{\mathbf{u}} \hat{\mathbf{y}}_k(t)\|_2,$$

where $\hat{\mathbf{y}}_k(t) = \text{vec}(\widehat{\mathbf{Y}}_k(t))$ solves the reduced problem $\hat{\mathbf{y}}_k(t) = \mathbb{V}_{\mathbf{u}}^\top \mathbf{L} \mathbb{V}_{\mathbf{u}} \hat{\mathbf{y}}_k(t) + \mathbb{V}_{\mathbf{u}}^\top \mathbb{Q}_{\mathbf{f}} \mathbf{f}(\mathbb{V}_{\mathbf{u}} \hat{\mathbf{y}}_k, t)$.

For ETD applied to semilinear differential equations the additional requirement is that \mathbf{L}_k be sectorial, which can also be assumed for the discretization of the considered operator ℓ ; see [31, Th.4 for order $s = 1$]. The error in (7.2) can therefore be approximated by applying the a-priori [20] or a posteriori [53] error estimates to the vectorized system associated with $\hat{\mathbf{y}}_k$. Moreover, if $\mathbf{f}(\mathbf{u}, t)$ is Lipschitz continuous, this property is preserved by the reduced order vector model, since $\mathbb{V}_{\mathbf{u}}$ has orthonormal columns and $\|\mathbb{Q}_{\mathbf{f}}\|$ is a bounded constant, as shown in Proposition 6.1; see e.g., [20].

The complete 2S-POD-DEIM method for the semilinear differential problem (1.1) is presented in Algorithm 2S-POD-DEIM. In Table 1 we summarize the key dimensions and parameters of the whole procedure. A technical discussion of the algorithm and its computational complexity is postponed to Appendix A.

Algorithm 2S-POD-DEIM

INPUT: Coefficient matrices of (1.1), $\mathcal{F} : \mathbb{R}^{n \times n} \times [0, T_f] \rightarrow \mathbb{R}^{n \times n}$, (or its snapshots), n_{\max} , κ , and τ , n_t , $\{\mathbf{t}_i\}_{i=0, \dots, n_t}$.

OUTPUT: $\mathbf{V}_{\ell, \mathbf{U}}, \mathbf{W}_{r, \mathbf{U}}$ and $\mathbf{Y}_k^{(i)}$, $i = 0, \dots, n_t$ to implicitly form the approximation $\mathbf{V}_{\ell, \mathbf{U}} \mathbf{Y}_k^{(i)} \mathbf{W}_{r, \mathbf{U}}^\top \approx \mathbf{U}(t_i)$

Offline:

1. Determine $\mathbf{V}_{\ell, \mathbf{U}}, \mathbf{W}_{r, \mathbf{U}}$ for $\{\mathbf{U}\}_{i=1}^{n_{\max}}$ and $\mathbf{V}_{\ell, \mathcal{F}}, \mathbf{W}_{r, \mathcal{F}}$ for $\{\mathcal{F}\}_{i=1}^{n_{\max}}$ via Algorithm 5.1 (DYNAMIC 2S-POD) using at most n_s of the n_{\max} time instances (if not available, this includes approximating the snapshots $\{\mathcal{F}(t_i)\}_{i=1}^{n_{\max}}$, $\{\mathbf{U}(t_i)\}_{i=1}^{n_{\max}}$ as the time interval is spanned);
2. Compute $\mathbf{Y}_k^{(0)} = \mathbf{V}_{\ell, \mathbf{U}}^\top \mathbf{U}_0 \mathbf{W}_{r, \mathbf{U}}$, $\mathbf{A}_k = \mathbf{V}_{\ell, \mathbf{U}}^\top \mathbf{A} \mathbf{V}_{\ell, \mathbf{U}}$, $\mathbf{B}_k = \mathbf{W}_{r, \mathbf{U}}^\top \mathbf{B} \mathbf{W}_{r, \mathbf{U}}$;
3. Determine $\mathbf{P}_{\ell, \mathcal{F}}, \mathbf{P}_{r, \mathcal{F}}$ using q-deim(2S-DEIM);
4. Compute $\mathbf{V}_{\ell, \mathbf{U}}^\top \mathbf{V}_{\ell, \mathcal{F}} (\mathbf{P}_{\ell, \mathcal{F}}^\top \mathbf{V}_{\ell, \mathcal{F}})^{-1}$, $(\mathbf{W}_{r, \mathcal{F}}^\top \mathbf{P}_{r, \mathcal{F}})^{-1} \mathbf{W}_{r, \mathcal{F}}^\top \mathbf{W}_{r, \mathbf{U}}$, $\mathbf{P}_{\ell, \mathcal{F}}^\top \mathbf{V}_{\ell, \mathbf{U}}$ and $\mathbf{W}_{r, \mathbf{U}}^\top \mathbf{P}_{r, \mathcal{F}}$;

Online:

5. For each $i = 1, \dots, n_t$
 - (i) Evaluate $\mathcal{F}_k(\mathbf{Y}_k^{(i-1)}, \mathbf{t}_{i-1})$ as in (6.5) using the matrices computed above;
 - (ii) Numerically solve the matrix equation (7.1) and compute

$$\mathbf{Y}_k^{(i)} = e^{h\mathbf{A}_k} \mathbf{Y}_k^{(i-1)} e^{h\mathbf{B}_k} + h\Phi^{(i-1)};$$

8. Numerical experiments. In this section we illustrate the performance of our matrix-oriented 2S-POD-DEIM integrator. In section 8.1 we analyze the quality of the approximation space created by the DYNAMIC algorithm on three nonlinear functions with different characteristics. Then in section 8.2 we focus on the ODE setting by comparing the new 2S-POD-DEIM procedure to the standard POD-DEIM.

8.1. Approximation of a nonlinear function \mathcal{F} . We investigate the effectiveness of the proposed DYNAMIC 2S-POD procedure for determining the two-sided approximation space of a nonlinear function.

Table 1: Summary of leading dimensions and parameters of Algorithm 2S-POD-DEIM.

Par.	Description
n_s	Employed number of snapshots
k	Dimension of vector POD subspace
p	Dimension of vector DEIM approx. space
N	Length of $\mathbf{u}(t)$, $N = n^2$.
κ	Dimension of the snapshot space approximation
k_i	Dimension of left ($i = 1$) and right ($i = 2$) 2S-POD subspaces
p_i	Dimension of left ($i = 1$) and right ($i = 2$) 2S-DEIM subspaces
n	Dimension of square $\mathbf{U}(t)$, for $n = n_x = n_y$

As a reference comparison, we consider the vector form of the DEIM approximation (hereafter VECTOR) in section 2.

We also include comparisons with a simple two-sided matrix reduction strategy that uses a sequential evaluation of all available snapshots, together with the updating of the bases $\mathbf{V}_{\ell, \mathcal{F}}$ and $\mathbf{W}_{r, \mathcal{F}}$ during the snapshot processing. In particular, if $[\mathbf{V}_j, \boldsymbol{\Sigma}_j, \mathbf{W}_j] = \text{svds}(\mathcal{F}_j, \kappa)$ is the singular value decomposition of \mathcal{F}_j limited to the leading κ singular triplets, then in this simple approach the basis matrices $\mathbf{V}_{\ell, \mathcal{F}}$ and $\mathbf{W}_{r, \mathcal{F}}$ are directly updated by orthogonal reduction of the augmented matrices

$$(8.1) \quad \left(\mathbf{V}_{\ell, \mathcal{F}}, \mathbf{V}_j \boldsymbol{\Sigma}_j^{\frac{1}{2}} \right) \in \mathbb{R}^{n \times \kappa_1} \quad \text{and} \quad \left(\mathbf{W}_{r, \mathcal{F}}, \mathbf{W}_j \boldsymbol{\Sigma}_j^{\frac{1}{2}} \right) \in \mathbb{R}^{n \times \kappa_2}$$

respectively, where $\kappa_1, \kappa_2 \geq \kappa$. To make this procedure comparable in terms of memory to Algorithm 3.1, we enforce that the final dimension ν_j of each basis satisfies $\nu_j \leq \kappa$, for $j = \ell, r$. We will refer to this as the VANILLA procedure for adding a snapshot to the approximation space; see, for instance, [43], [33] for additional details.

EXAMPLE 1. Consider the nonlinear functions $\phi_i : \Omega \times [0, T_f] \rightarrow \mathbb{R}$, $\Omega \subset \mathbb{R}^2$, $i = 1, 2, 3$ defined as

$$\begin{cases} \phi_1(x_1, x_2, t) = \frac{x_2}{\sqrt{(x_1+x_2-t)^2 + (2x_1-3t)^2 + 0.01^2}}, & \Omega = [0, 2] \times [0, 2], T_f = 2, \\ \phi_2(x_1, x_2, t) = \frac{x_1 x_2}{(x_2 t + 0.1)^2} + \frac{2(x_1+x_2)}{\sqrt{(x_1+x_2-t)^2 + (x_2^2+x_1^2-t^2)^2 + 0.01^2}}, & \Omega = [0, 1] \times [0, 1.5], T_f = 3, \\ \phi_3(x_1, x_2, t) = \frac{x_1(0.1+t)}{(x_2 t + 0.1)^2} + \frac{t 2(x_1+x_2)}{\sqrt{(x_1+x_2-t)^2 + (x_2^2+x_1^2-3t)^2 + 0.01^2}}, & \Omega = [0, 3] \times [0, 3], T_f = 5. \end{cases}$$

Each function is discretized with $n = 2000$ nodes in each spatial direction to form three matrix valued functions $\mathcal{F}^{(i)} : [0, T_f] \rightarrow \mathbb{R}^{n \times n}$, for $i = 1, \dots, 3$, respectively. In the truncation criterion (3.7), for all functions we set $n_{max} = 60$ and $\tau = 10^{-3}$. The function ϕ_1 shows significant variations at the beginning of the time window, ϕ_3 varies more towards the right-hand of the time span, while ϕ_2 is somewhere in between.

The approximations obtained with the considered methods are reported in Table 2 for $\kappa = 50$ and $\kappa = 70$, with the following information: For the adaptive snapshot selection procedure, we indicate the required number of PHASES and the final total number n_s of snapshot used, the CPU time to construct the basis vectors (time for Algorithm 3.1 plus time for the SVDs (8.1) or VANILLA), the final dimensions ν_ℓ and ν_r and finally, the arithmetic mean of the errors $\|\mathcal{F}(t_j) - \mathbf{V}_{\ell, \mathcal{F}} \mathbf{V}_{\ell, \mathcal{F}}^\top \mathcal{F}(t_j) \mathbf{W}_{r, \mathcal{F}} \mathbf{W}_{r, \mathcal{F}}^\top\| / \|\mathcal{F}(t_j)\|$ over 300 equispaced timesteps t_j , for each $\mathcal{F} = \mathcal{F}^{(i)}$, $i = 1, 2, 3$. For the vector approach, where we used $n_s = \kappa$, the reported time consists of the CPU time needed

to perform the SVD of the long snapshots, while the error is measured using the vector form corresponding to the formula above; see the description at the beginning of section 8.2.

Ξ	alg.	$\kappa = 50$				$\kappa = 70$			
		phases (n_s)	time sec.	ν_ℓ/ν_r	error	phases (n_s)	time sec.	ν_ℓ/ν_r	error
f_1	DYNAMIC	2 (9)	3.5	33/39	$6 \cdot 10^{-4}$	1(7)	4.7	40/50	$3 \cdot 10^{-4}$
	VANILLA	-(60)	27.6	42/50	$6 \cdot 10^{-4}$	-(60)	38.8	42/60	$3 \cdot 10^{-4}$
	VECTOR	-(50)	35.9	41	$1 \cdot 10^{-3}$	-(70)	77.3	56	$3 \cdot 10^{-4}$
f_2	DYNAMIC	3(21)	8.6	45/26	$8 \cdot 10^{-4}$	2(10)	6.1	48/30	$6 \cdot 10^{-4}$
	VANILLA	-(60)	25.6	50/37	$4 \cdot 10^{-4}$	-(60)	39.6	58/37	$2 \cdot 10^{-4}$
	VECTOR	-(50)	42.7	36	$6 \cdot 10^{-3}$	-(70)	91.8	47	$2 \cdot 10^{-3}$
f_3	DYNAMIC	2(11)	4.4	34/33	$1 \cdot 10^{-3}$	1(10)	5.9	39/39	$3 \cdot 10^{-4}$
	VANILLA	-(60)	25.4	46/46	$2 \cdot 10^{-4}$	-(60)	38.6	46/46	$2 \cdot 10^{-4}$
	VECTOR	-(50)	47.1	50	$2 \cdot 10^{-3}$	-(70)	92.5	64	$8 \cdot 10^{-4}$

Table 2: Example 1. Performance of DYNAMIC, VANILLA and VECTOR algorithms for $n = 2000$.

Between the matrix-oriented procedures, the dynamic procedure outperforms the simplified one, both in terms of space dimensions n_s , ν_ℓ and ν_r , and in terms of CPU time, especially when not all time selection phases are needed. The error is comparable for the two methods. Not unexpectedly, increasing κ allows one to save on the number of snapshots n_s , though a slightly larger reduced dimension ν_ℓ/ν_r may occur. The vector method is not competitive for any of the observed parameters, taking into account that vectors of length n^2 need be stored. \square

8.2. Solution approximation of the full problem. We report on a selection of numerical experiments with the DYNAMIC 2S-POD-DEIM procedure on matrix semi-linear differential equations of the form (1.1). Once again, we compare the results with a standard vector procedure that applies standard POD-DEIM to the vectorized solution and nonlinear function snapshots. In particular, we apply the (vectorized) adaptive procedure from section 5 using the error $\|\xi - V_k V_k^T \xi\|/\|\xi\|$ for the selection criterion, where ξ is the vectorized snapshot and V_k is the existing POD basis. Notice that in the vector setting we need to process as many nodes, as the final space dimension, which depends on the tolerance τ . This is due to the fact that no reduction takes place.

In all experiments CPU times are in seconds, and all bases are truncated using the criterion in (3.7). To illustrate the quality of the obtained numerical solution, we also report on the evaluation of the following average relative error norm

$$(8.2) \quad \bar{\mathcal{E}}(\mathbf{U}) = \frac{1}{n_t} \sum_{\gamma=1}^{n_t} \frac{\|\mathbf{U}^{(j)} - \tilde{\mathbf{U}}^{(j)}\|_F}{\|\mathbf{U}^{(j)}\|_F},$$

where $\tilde{\mathbf{U}}^{(j)}$ represents either the DYNAMIC approximation, or the matricization of the VECTOR approximation and $\mathbf{U}^{(j)}$ is determined by means of the exponential Euler method applied to the original problem.

Table 3 shows the key numbers for the bases construction for both methods. For either \mathbf{U} or \mathcal{F} we report the number of PHASES, the number n_s of included snapshots, and the final space dimensions after the reduction procedure. We first describe the considered model problem and then comment on the numbers in Table 3 and on

the detailed analysis illustrated in Table 4. We stress that these may be considered typical benchmark problems for our problem formulation. We also remark that for some of the experimental settings the problem becomes symmetric, so that thanks to Remark 3.1 the two bases could be taken to be the same with further computational and memory savings. Nonetheless, we do not exploit this extra feature in the reported experiments.

For all examples the full matrix problem has dimension $n = 1000$, while the selected values for κ , n_{\max} and n_t are displayed in Table 3 and Table 4, respectively.

EXAMPLE 2. *The 2D Allen-Cahn equation [1].* Consider the equation⁴

$$(8.3) \quad u_t = \epsilon_1 \Delta u - \frac{1}{\epsilon_2} (u^3 - u), \quad \Omega = [a, b]^2, \quad t \in [0, T_f],$$

with initial condition $u(x, y, 0) = u_0$. The first example is referred to as AC 1. As in [47], we use the following problem parameters: $\epsilon_1 = 10^{-2}$, $\epsilon_2 = 1$, $a = 0$, $b = 2\pi$ and $T_f = 5$. Finally, we set $u_0 = 0.05 \sin x \cos y$ and impose homogeneous Dirichlet boundary conditions. The second problem (hereafter AC 2) is a mean curvature flow problem ([24]) of the form (8.3) with data as suggested, e.g., in [32, Section 5.2.2], that is periodic boundary conditions, $\epsilon_1 = 1$, $a = -0.5$, $b = 0.5$, $T_f = 0.075$, with $u_0 = \tanh\left(\frac{0.4 - \sqrt{x^2 + y^2}}{\sqrt{2}\epsilon_2}\right)$. Following [32, Section 5.2.2] we consider $\epsilon_2 \in \{0.01, 0.02, 0.04\}$. As ϵ_2 decreases stability reasons enforce the use of finer time discretizations n_t , also leading to larger values of n_{\max} and κ , as indicated in Table 3 and Table 4, where we report our experimental results. \square

EXAMPLE 3. *Reaction-convection-diffusion equation.* We consider the following reaction-convection-diffusion (hereafter RCD) problem, also presented in [17],

$$(8.4) \quad u_t = \epsilon_1 \Delta u + (u_x + u_y) + u(u - 0.5)(1 - u), \quad \Omega = [0, 1]^2, \quad t \in [0, 0.3].$$

The initial solution is given by $u_0 = 0.3 + 256(x(1-x)y(1-y))^2$, while zero Neumann boundary conditions are imposed. In Table 3 and Table 4 we present results for $\epsilon_1 \in \{0.5, 0.05\}$. \square

Table 3 shows that for both the solution and the nonlinear function snapshots, the DYNAMIC procedure requires merely one phase, and it retains snapshots at only a few of the time instances. On the other hand, the vector approach typically requires two or even three phases to complete the procedure. The dimension of the bases is not comparable for the matrix and vector approaches, since these are subspaces of spaces of significantly different dimensions, namely \mathbb{R}^n and \mathbb{R}^{n^2} in the matrix and vector cases, respectively. Nonetheless, it is clear that the memory requirements are largely in favor of the matrix approach, as shown in Table 4, where computational and memory details are reported. In particular, in Table 4 the offline timings are broken down into two main parts. The column BASIS TIME collects the cost of the Gram-Schmidt orthogonalization in the VECTOR setting, and the cumulative cost of Algorithm 3.1 (for both the solution and nonlinear function snapshots) for the DYNAMIC procedure. Column DEIM TIME reports the time required to determine the interpolation indices by `q-deim`. The “online times” report the cost to simulate both reduced order models at n_t timesteps. The relative approximation error in (8.2) is also displayed, together with the total memory requirements for the offline and online

⁴Note that the linear term $-u$ is kept in the nonlinear part of the operator.

Table 3: **Example 2:** Performance of DYNAMIC and VECTOR algorithms for $n = 1000$.

PB.	n_{\max}/κ	Ξ	ALGORITHM	PHASES	n_s	ν_ℓ/ν_r
AC 1	40/50	\mathcal{U}	DYNAMIC	1	8	9/2
			VECTOR	2	9	9
		\mathcal{F}	DYNAMIC	1	7	10/3
			VECTOR	2	9	9
AC 2 $\epsilon_2 = 0.04$	400/50	\mathcal{U}	DYNAMIC	1	2	15/15
			VECTOR	2	25	25
		\mathcal{F}	DYNAMIC	1	3	27/27
			VECTOR	2	40	40
AC 2 $\epsilon_2 = 0.02$	1200/70	\mathcal{U}	DYNAMIC	1	3	30/30
			VECTOR	1	28	28
		\mathcal{F}	DYNAMIC	1	4	39/39
			VECTOR	2	53	53
AC 2 $\epsilon_2 = 0.01$	5000/150	\mathcal{U}	DYNAMIC	1	3	62/62
			VECTOR	1	43	43
		\mathcal{F}	DYNAMIC	1	5	73/73
			VECTOR	2	92	92
RDC $\epsilon_1 = 0.5$	60/50	\mathcal{U}	DYNAMIC	1	3	10/10
			VECTOR	1	7	7
		\mathcal{F}	DYNAMIC	1	3	13/13
			VECTOR	2	11	11
RDC $\epsilon_1 = 0.05$	60/50	\mathcal{U}	DYNAMIC	1	4	14/14
			VECTOR	3	14	14
		\mathcal{F}	DYNAMIC	1	3	17/17
			VECTOR	3	34	34

parts. In terms of memory, for the VECTOR setting this includes the storage of all the processed snapshots while for 2S-POD-DEIM that of $\tilde{\mathbf{V}}_i$ and $\tilde{\mathbf{W}}_i$ from [Algorithm 3.1](#), for both the solution and nonlinear function snapshots. This quantity is always equal to $4\kappa \cdot n$ for the DYNAMIC setting.

We point out the large gain in basis construction time for the DYNAMIC procedure, mainly related to the low number of snapshots employed (cf. [Table 3](#)). Furthermore, the DYNAMIC procedure enjoys a massive gain in memory requirements, for very comparable online time and final average errors.

For the reaction-convection-diffusion example we also analyze the dependence of the number n_s of retained snapshots on the threshold τ of the two procedures, having fixed $n_{\max} = 60$. For the vector procedure n_s increases as the tolerance τ decreases, whereas for the dynamic procedure n_s remains nearly constant for changing τ . This ultimately indicates that the offline cost will increase for the VECTOR procedure, if a richer basis is required; see the appendix and [Table 5](#) for a detailed discussion.

9. Conclusions and future work. We have proposed a matrix-oriented POD-DEIM type order reduction strategy to efficiently handle the numerical solution of semilinear matrix differential equations in two space variables. By introducing a novel interpretation of the proper orthogonal decomposition when applied to functions in two variables, we devised a new two-sided discrete interpolation strategy that is also able to preserve the symmetric structure in the original nonlinear function and in the approximate solution. The numerical treatment of the matrix reduced order differential problem can take full advantage of both the small dimension and the matrix setting, by exploiting effective exponential integrators. Our very encouraging numerical experiments show that the new procedure can dramatically decrease memory and

Table 4: Computational time and storage requirements of 2S-POD-DEIM and standard vector POD-DEIM. CPU times are in seconds and $n = 1000$.

PB.	METHOD	OFFLINE			ONLINE		REL. ERROR
		BASIS TIME	DEIM TIME	MEMORY	TIME (n_t)	MEMORY	
AC 1	DYNAMIC	1.8	0.001	$200n$	0.009 (300)	$24n$	$1 \cdot 10^{-4}$
	VECTOR	0.6	0.228	$18n^2$	0.010 (300)	$18n^2$	$1 \cdot 10^{-4}$
AC 2 0.04	DYNAMIC	0.8	0.005	$200n$	0.010 (300)	$84n$	$3 \cdot 10^{-4}$
	VECTOR	8.4	3.745	$65n^2$	0.020 (300)	$65n^2$	$2 \cdot 10^{-4}$
AC 2 0.02	DYNAMIC	1.8	0.004	$280n$	0.140 (1000)	$138n$	$2 \cdot 10^{-4}$
	VECTOR	14.56	5.273	$81n^2$	0.120 (1000)	$81n^2$	$3 \cdot 10^{-5}$
AC 2 0.01	DYNAMIC	5.3	0.008	$600n$	0.820 (2000)	$270n$	$5 \cdot 10^{-4}$
	VECTOR	46.2	13.820	$135n^2$	0.420 (2000)	$135n^2$	$2 \cdot 10^{-4}$
RDC 0.5	DYNAMIC	0.8	0.001	$200n$	0.008 (300)	$46n$	$2 \cdot 10^{-4}$
	VECTOR	0.6	0.277	$18n^2$	0.010 (300)	$18n^2$	$1 \cdot 10^{-4}$
RDC 0.05	DYNAMIC	0.9	0.001	$200n$	0.010 (300)	$62n$	$2 \cdot 10^{-4}$
	VECTOR	4.1	2.297	$48n^2$	0.010 (300)	$48n^2$	$1 \cdot 10^{-4}$

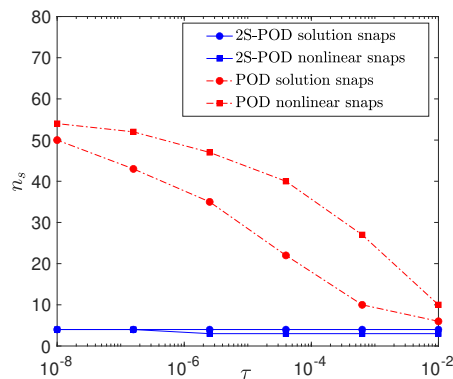


Fig. 8.1: Example 3. $n = 1000$. Number of retained snapshots with respect to τ , for $\epsilon_1 = 0.05$.

CPU time requirements for the function reduction procedure in the so-called offline phase. Moreover, we illustrated that the reduced low-dimensional matrix differential equation can be numerically solved in a rapid online phase, without sacrificing too much accuracy.

This work can be expanded in various directions. In particular, the companion paper [33] presents a first experimental exploration of the three dimensional case, which takes advantage of the tensor setting, and uses recently developed tensor linear equations solvers to advance in time in the (tensor) reduced differential equation; a dynamic approach could enhance the implementation in [33]. Generalizations to the multidimensional case and to multiparameters suggest themselves.

Acknowledgments. The authors are members of Indam-GNCS, which support is gratefully acknowledged. Part of this work was also supported by the Grant AlmaIdea 2017-2020 - Università di Bologna.

Appendix A. Discussion of 2S-POD-DEIM algorithm and computational complexity. We compare the computational complexity of the new 2S-POD-DEIM method applied to (1.1) with that of standard POD-DEIM. All discussions are related to Algorithm 2S-POD-DEIM in section 7.

The offline phase. The first part of the presented algorithm defines the offline phase. For the \mathbf{U} -set, we considered the semi-implicit Euler scheme applied directly to the differential equation in *matrix* form; see, e.g., [21], whereas the snapshot selection is done via the adaptive procedure discussed in section 5. Notice that moving from one PHASE to the next in Algorithm 5.1 does not require recomputing any quantities. Indeed, if h^* is the stepsize of the new phase, we determine $\mathbf{U}(h^*)$ from $\mathbf{U}(0)$ and initialize the semi-implicit Euler scheme from there; see also Figure 5.1.

The computational complexity of approximating the κ leading singular triplets with `svds`, as required by Algorithm 3.1 is given by the implicitly restarted Lanczos bidiagonalization, as implemented in the matlab function `svds`. For each i this cost is mainly given by matrix vector multiplications with the dense $n \times n$ matrix; one Arnoldi cycle involves at most 2κ such products, together with 2κ basis orthogonalizations, leading to $\mathcal{O}(n^2\kappa + n\kappa)$ operations per cycle [7]. The final SVDs for *bases pruning* at the end of Algorithm 5.1 are performed with a dense solver, and each has complexity $\mathcal{O}(11\kappa^3)$ [26, p.493]. Furthermore, each skinny QR -factorization required for the projections Π_ℓ and Π_r in (5.1) has complexity $\mathcal{O}(2n\kappa^2)$ [26, p.255]. For the standard POD-DEIM algorithm, the reported SVD complexity is the total cost of orthogonalizing all selected snapshots by means of Gram-Schmidt, which is $\mathcal{O}(Nn_s^2)$.

The projected coefficient matrices \mathbf{A}_k , \mathbf{B}_k , and \mathbf{Y}_0 are computed once for all and stored in step 2 of Algorithm 2S-POD-DEIM, with a total complexity of approximately $\mathcal{O}(n^2(k_1 + k_2) + n(k_1 + k_2 + k_1^2 + k_2^2))$, assuming that \mathbf{A} and \mathbf{B} are sparse and \mathbf{U}_0 is dense. This step is called POD projection in Table 5.

Step 3 in the Algorithm 2S-POD-DEIM has a computational complexity of $\mathcal{O}(n(p_1^2 + p_2^2))$ [23], while the matrices in step 4 need to be computed and stored with computational complexity $\mathcal{O}(n(k_1 + k_2)(p_1 + p_2) + (p_1^2 + p_2^2)n + p_1^3 + p_2^3)$ in total [19]. This step is called DEIM projection in Table 5. We recall that the products involving the selection matrices $\mathbf{P}_{\ell,\mathcal{F}}$ and $\mathbf{P}_{r,\mathcal{F}}$ do not entail any computation.

Finally, for the ETD we report the costs for the reduced procedure described in [21, Section 3.3], since we did not experience any stability issues with the diagonalization in our experiments. To this end an a-priori spectral decomposition of each of the reduced matrices \mathbf{A}_k and \mathbf{B}_k is done once for all, which has complexity $\mathcal{O}(9k_1^3 + 9k_2^3)$ for dense symmetric⁵ matrices [26]. This makes the cost of evaluating the matrix exponentials negligible, since the computations at each time iteration online will be performed within the eigenbases, following [21, Section 3.3]. Furthermore, thanks to the small dimension of the matrices we also explicitly compute the inverse of the eigenvector matrices at a cost of $\mathcal{O}(k_1^3 + k_2^3)$, as required by the online computation.

All these costs are summarized in Table 5 and compared with those of the standard POD-DEIM offline phase applied to (1.6), as indicated in [19], with dimension $N = n^2$. All coefficient matrices are assumed to be sparse and it is assumed that both methods

⁵If the coefficient matrices were nonsymmetric, this will be more expensive (still of cubic order), but determining the exact cost is however still an open problem [26].

select n_s snapshots via the adaptive procedure. In practice, however, it appears that the two-sided procedure requires far fewer snapshots than the vectorization procedure, as indicated by Table 3. The table also includes the memory requirements for the snapshots and the basis matrices.

Table 5: Offline phase: Computational costs (flops) for standard POD-DEIM applied to (1.6), and 2S-POD-DEIM applied to (1.1), and principal memory requirements. Here $N = n^2$.

Procedure	POD-DEIM	DYNAMIC 2S-POD-DEIM
SVD	$\mathcal{O}(Nn_s^2)$	$\mathcal{O}(n^2\kappa n_s + n\kappa n_s + 6n\kappa^2 + 11\kappa^3)$
QR	–	$\mathcal{O}(n\kappa^2 n_s)$
DEIM	$\mathcal{O}(Np^2)$	$\mathcal{O}(n(p_1^2 + p_2^2))$
POD projection	$\mathcal{O}(Nk + Nk^2)$	$\mathcal{O}(n^2(k_1 + k_2) + n(k_1 + k_2 + k_1^2 + k_2^2))$
DEIM projection	$\mathcal{O}(Nkp + p^2N + p^3)$	$\mathcal{O}(n(k_1 + k_2)(p_1 + p_2) + (p_1^2 + p_2^2)n + p_1^3 + p_2^3)$
Snapshot Storage	$\mathcal{O}(Nn_s)$	$\mathcal{O}(n\kappa)$
Basis Storage	$\mathcal{O}(N(k + p))$	$\mathcal{O}(n(k_1 + k_2 + p_1 + p_2))$

The online phase. The total cost of performing step 5.(i) is $\mathcal{O}(\omega(p_1p_2) + k_1p_1p_2 + k_1k_2p_2)$, where $\omega(p_1p_2)$ is the cost of evaluating the nonlinear function at p_1p_2 entries. Step 5.(ii) requires a matrix–matrix product and the solution of the Sylvester equation (7.1) in the eigenspace. The latter demands only matrix–matrix products, which come at a cost of $\mathcal{O}(k_1^2k_2 + k_1k_2^2)$ and two Hadamard products with complexity $\mathcal{O}(k_1k_2)$; see [21] for more details. This brings the total complexity of one time iteration online to $\mathcal{O}(\omega(p_1p_2) + k_1p_1p_2 + k_1k_2p_2 + k_1^2k_2 + k_1k_2^2 + k_1k_2)$, which is independent of the original problem size n .

REFERENCES

- [1] S. M. ALLEN AND J. W. CAHN, *A microscopic theory for antiphase boundary motion and its application to antiphase domain coarsening*, Acta Metall, 27 (1979), pp. 1085–1095.
- [2] D. AMSALLEM AND C. FARHAT, *An online method for interpolating linear parametric reduced-order models*, SIAM J. Sci. Comput., 33 (2011), pp. 2169–2198.
- [3] H. ANTIL, M. HEINKENSCHLOSS, AND D. C. SORENSEN, *Application of the discrete empirical interpolation method to reduced order modeling of nonlinear and parametric systems*, in Reduced order methods for modeling and computational reduction, Springer, 2014, pp. 101–136.
- [4] A. ANTOULAS, C. BEATTIE, AND S. GUGERCIN, *Interpolatory methods for model reduction*, SIAM, Philadelphia, 2020.
- [5] U. M. ASCHER, S. J. RUUTH, AND B. T. WETTON, *Implicit-explicit methods for time-dependent partial differential equations*, SIAM J. Numer. Anal., 32 (1995), pp. 797–823.
- [6] P. ASTRID, S. WEILAND, K. WILLCOX, AND T. BACKX, *Missing point estimation in models described by proper orthogonal decomposition*, IEEE Trans. Autom. Control, 53 (2008), pp. 2237–2251.
- [7] J. BAGLAMA AND L. REICHEL, *Augmented implicitly restarted Lanczos bidiagonalization methods*, SIAM J. Sci. Comput., 27 (2005), pp. 19–42.
- [8] M. BARRAULT, Y. MADAY, N. C. NGUYEN, AND A. T. PATERA, *An ‘empirical interpolation’ method: application to efficient reduced-basis discretization of partial differential equations*, C. R. Math. Acad. Sci. Paris, 339 (2004), pp. 667–672.
- [9] R. H. BARTELS AND G. W. STEWART, *Solution of the matrix equation $AX + XB = C$ [F_4]*, Commun. ACM, 15 (1972), pp. 820–826.
- [10] M. BEHR, P. BENNER, AND J. HEILAND, *Solution formulas for differential Sylvester and Lyapunov equations*, Calcolo, 56:51 (2019).

- [11] P. BENNER AND T. BREITEN, *Two-sided projection methods for nonlinear model order reduction*, SIAM J. Sci. Comput., 37 (2015), pp. B239–B260.
- [12] P. BENNER, S. GUGERCIN, AND K. WILLCOX, *A survey of projection-based model reduction methods for parametric dynamical systems*, SIAM Rev, 57 (2015), pp. 483–531.
- [13] P. BENNER, V. MEHRMANN, AND D. SORESENSEN, *Dimension reduction of large-scale systems*, Springer-Verlag, Berlin/Heidelberg, Germany, 2005.
- [14] P. BENNER, M. OHLBERGER, A. COHEN, AND K. WILLCOX, *Model reduction and approximation: theory and algorithms*, SIAM, Philadelphia, 2017.
- [15] D. BONOMI, A. MANZONI, AND A. QUARTERONI, *A matrix DEIM technique for model reduction of nonlinear parametrized problems in cardiac mechanics*, Comput. Methods Appl. Mech. Eng., 324 (2017), pp. 300–326.
- [16] M. BRACHET, L. DEBREU, AND C. ELDRD, *Comparison of exponential integrators and traditional time integration schemes for the shallow water equations*, hal-02479047v2, (2020).
- [17] M. CALIARI AND A. OSTERMANN, *Implementation of exponential Rosenbrock-type integrators*, Applied Numerical Mathematics, 59 (2009), pp. 568–581.
- [18] K. CARLBERG, R. TUMINARO, AND P. BOGGS, *Preserving Lagrangian structure in nonlinear model reduction with application to structural dynamics*, SIAM J. Sci. Comput., 37 (2015), pp. B153–B184.
- [19] S. CHATURANTABUT AND D. C. SORESENSEN, *Nonlinear model reduction via discrete empirical interpolation*, SIAM J. Sci. Comput., 32 (2010), pp. 2737–2764.
- [20] ———, *A state space error estimate for POD-DEIM nonlinear model reduction*, SIAM J Numer Anal, 50 (2012), pp. 46–63.
- [21] M. C. D’AUTILIA, I. SGURA, AND V. SIMONCINI, *Matrix-oriented discretization methods for reaction–diffusion PDEs: Comparisons and applications*, Computers & Mathematics with Applications, (2020), pp. 2067–2085.
- [22] R. DEDDEN, *Model order reduction using the discrete empirical interpolation method*, Master’s thesis, TU Delft, 2012.
- [23] Z. DRMAČ AND S. GUGERCIN, *A new selection operator for the discrete empirical interpolation method—improved a priori error bound and extensions*, SIAM J. Sci. Comput., 38 (2016), pp. A631–A648.
- [24] L. C. EVANS AND J. SPRUCK, *Motion of level sets by mean curvature. I*, J. Differ. Geom., 33 (1991), pp. 635–681.
- [25] F. GARCIA, L. BONAVENTURA, M. NET, AND J. SÁNCHEZ, *Exponential versus IMEX high-order time integrators for thermal convection in rotating spherical shells*, J. Comput. Phys., 264 (2014), pp. 41–54.
- [26] G. H. GOLUB AND C. F. VAN LOAN, *Matrix Computations*, Johns Hopkins University Press, Baltimore, fourth ed., 2013.
- [27] I. GROOMS AND K. JULIEN, *Linearly implicit methods for nonlinear PDEs with linear dispersion and dissipation*, J. Comput. Phys., 230 (2011), pp. 3630–3650.
- [28] C. GU, *QLMOR: A projection-based nonlinear model order reduction approach using quadratic-linear representation of nonlinear systems*, IEEE Trans. Comput.-Aided Design Integr. Circuits Syst., 30 (2011), pp. 1307–1320.
- [29] N. J. HIGHAM, *Functions of matrices: theory and computation*, SIAM, Philadelphia, 2008.
- [30] M. HINZE AND S. VOLKWEIN, *Proper orthogonal decomposition surrogate models for nonlinear dynamical systems: Error estimates and suboptimal control*, in Dimension reduction of large-scale systems, Springer, 2005, pp. 261–306.
- [31] M. HOCHBRUCK AND A. OSTERMANN, *Explicit exponential Runge–Kutta methods for semilinear parabolic problems*, SIAM J. Numer. Anal., 43 (2005), pp. 1069–1090.
- [32] L. JU, J. ZHANG, L. ZHU, AND Q. DU, *Fast explicit integration factor methods for semilinear parabolic equations*, J. Sci. Comput., 62 (2015), pp. 431–455.
- [33] G. KIRSTEN, *Multilinear POD-DEIM model reduction for 2D and 3D nonlinear systems of differential equations*, arXiv preprint arXiv:2103.04343, (2021).
- [34] G. KIRSTEN AND V. SIMONCINI, *A matrix-oriented POD-DEIM algorithm applied to nonlinear differential matrix equations*, 2020. arXiv 2006.13289.
- [35] G. KIRSTEN AND V. SIMONCINI, *Order reduction methods for solving large-scale differential matrix Riccati equations*, SIAM J. Sci. Comput., 42 (2020), pp. A2182–A2205.
- [36] B. KRAMER AND K. E. WILLCOX, *Nonlinear model order reduction via lifting transformations and proper orthogonal decomposition*, AIAA Journal, 57 (2019), pp. 2297–2307.
- [37] K. KUNISCH AND S. VOLKWEIN, *Control of the Burgers equation by a reduced-order approach using proper orthogonal decomposition*, J. Optim. Theory Appl., 102 (1999), pp. 345–371.
- [38] P. K. MAINI AND H. G. OTHMER, *Mathematical Models for Biological Pattern Formation*, The IMA Volumes in Mathematics and its Applications - Frontiers in application of Mathemat-

- ics, Springer-Verlag, New York, 2001.
- [39] H. MALCHOW, S. PETROVSKII, AND E. VENTURINO, *Spatiotemporal Patterns in Ecology and Epidemiology: Theory, Models, and Simulations*, Chapman & Hall, CRC, London, 2008.
 - [40] THE MATHWORKS, *MATLAB 7*, r2013b ed., 2013.
 - [41] F. NEGRI, A. MANZONI, AND D. AMSALLEM, *Efficient model reduction of parametrized systems by matrix discrete empirical interpolation*, J. Comput. Phys., 303 (2015), pp. 431–454.
 - [42] N.-C. NGUYEN, A. T. PATERA, AND J. PERAIRE, *A ‘best points’ interpolation method for efficient approximation of parametrized functions*, Int J Numer Methods Eng, 73 (2008), pp. 521–543.
 - [43] G. M. OXBERRY¹, T. KOSTOVA-VASSILEVSKA, W. ARRIGHI, AND K. CHAND, *Limited-memory adaptive snapshot selection for proper orthogonal decomposition*, Int. J. Numer. Meth. Engng, 109 (2017), pp. 198–217.
 - [44] A. T. PATERA AND G. ROZZA, *Reduced basis approximation and a posteriori error estimation for parametrized partial differential equations*, MIT Cambridge, MA, USA, 2007.
 - [45] A. QUARTERONI, *Numerical Models for Differential Problems*, vol. 8 of MS&A - Modeling, Simulation and Applications, Springer-Verlag, Milan, 2017.
 - [46] V. SIMONCINI, *Computational methods for linear matrix equations*, SIAM Rev, 58 (2016), pp. 377–441.
 - [47] H. SONG, L. JIANG, AND Q. LI, *A reduced order method for Allen–Cahn equations*, J. Comput. Appl. Math., 292 (2016), pp. 213–229.
 - [48] D. C. SORENSEN AND M. EMBREE, *A DEIM induced CUR factorization*, SIAM J. Sci. Comput., 38 (2016), pp. A1454–A1482.
 - [49] R. ȘTEFĂNESCU AND A. SANDU, *Efficient approximation of sparse Jacobians for time-implicit reduced order models*, Int. J. Numer. Methods Fluids, 83 (2017), pp. 175–204.
 - [50] P. TISO AND D. J. RIXEN, *Discrete empirical interpolation method for finite element structural dynamics*, in Topics in Nonlinear Dynamics, Volume 1, Springer, 2013, pp. 203–212.
 - [51] A. TVEITO, H. P. LANGTANGEN, B. F. NIELSEN, AND X. CAI, *Elements of Scientific Computing*, Texts in Computational Science and Engineering, Springer-Verlag, Berlin, 2010.
 - [52] J. K. WHITE, *A trajectory piecewise-linear approach to model order reduction of nonlinear dynamical systems*, PhD thesis, Massachusetts Institute of Technology, 2003.
 - [53] D. WIRTZ, D. C. SORENSEN, AND B. HAASDONK, *A posteriori error estimation for DEIM reduced nonlinear dynamical systems*, SIAM J. Sci. Comput., 36 (2014), pp. A311–A338.